

Fine-scale fluctuations of PM₁, PM_{2.5}, PM₁₀ and SO₂ concentrations caused by a prolonged volcanic eruption (Fagradalsfjall 2021, Iceland)

Rachel C. W. Whitty¹, Evgenia Ilyinskaya¹, Melissa A. Pfeffer², Ragnar H. Thrastarson², Þorsteinn Johannsson³, Sara Barsotti², Tjarda J. Roberts^{4,5}, Guðni M. Gilbert^{2,9}, Tryggvi Hjörvar², Anja Schmidt^{6,7,8}, Daniela Fecht¹⁰, Grétar G. Sæmundsson¹¹

¹COMET, Institute of Geophysics and Tectonics, School of Earth and Environment, University of Leeds, Leeds, LS2 9JT, United Kingdom

²Icelandic Meteorological Office, 150 Reykjavík, Iceland

³The Environment Agency of Iceland, 108 Reykjavík, Iceland

⁴CNRS UMR7328, Laboratoire de Physique et de Chimie de l'Environnement et de l'Espace, Université d'Orléans, Orléans, 45071, France

⁵LMD/IPSL, ENS, Université PSL, École Polytechnique, Institute Polytechnique de Paris, Sorbonne Université, CNRS, F-75005 Paris, France

⁶Yusuf Hamed Department of Chemistry, University of Cambridge, Cambridge, CB2 1EW, United Kingdom

⁷Institute of Atmospheric Physics (IPA), German Aerospace Centre (DLR), 82234 Oberpfaffenhofen, Germany

⁸Meteorological Institute, Ludwig Maximilian University of Munich, 80333 Munich, Germany

⁹Nox Medical, 150 Reykjavík, Iceland

¹⁰MRC Centre for Environment and Health, School of Public Health, Imperial College London, London, W12 0BZ, United Kingdom

¹¹Department of Research and Analysis, Icelandic Tourist Board, 101 Reykjavík, Iceland

Correspondence to: Evgenia Ilyinskaya (e.ilyinskaya@leedss.ac.uk)

25

Abstract.

The 2021 Fagradalsfjall eruption marked the first in a series of ongoing eruptions in a densely populated region of Iceland (> 260,000 residents within 50 km distance). This eruption was monitored by an exceptionally dense regulatory air quality network, providing a unique opportunity to examine fine-scale dispersion patterns of volcanic air pollutants (SO₂, PM₁, PM_{2.5}, PM₁₀) in populated areas.

Despite its relatively small size, the eruption led to statistically-significant increases in both average and peak concentrations of PM and SO₂ at distances of at least 300 km. Peak daily-mean concentrations of PM₁ rose from 5–6 µg/m³ to 18–20 µg/m³,

and the proportion of PM₁ within PM₁₀ increased by ~50%. In areas with low background pollution, PM₁₀ and PM_{2.5} levels increased by ~50% but in places with high background sources, the eruption's impact was not detectable. These findings

35 suggest that ash-poor eruptions are a major source of PM₁ in Iceland and potentially in other regions exposed to volcanic emissions.

The 2021 Fagradalsfjall fissure eruption was the first of multiple ongoing eruptions in the most densely populated part of Iceland (70% of population within 50 km). It was monitored by an exceptionally dense reference-grade air quality network (14 stations within 40 km), and the first time that a reference-grade timeseries of PM₁ was collected during an eruption. We 40 used these measurements to investigate fine-scale dispersion patterns of volcanic air pollutants (SO₂, PM₁, PM_{2.5}, PM₁₀) in populated areas.

Air quality thresholds for all measured pollutants were exceeded more frequently during the eruption than under background 45 conditions. This suggests a possible increase in adverse health effects. Moreover, pollutant concentrations exhibited strong fine-scale temporal (<1 hour) and spatial (<1 km) variability. This suggests disparities in population exposures to volcanic air pollution, even from relatively distal sources (20–55 km distance), and underscores the importance of a dense monitoring network and effective public communication.

Despite its small size the eruption caused a statistically significant increase in average and peak PM and SO₂ concentrations 50 in at least 300 km distance. Peak daily means of PM₁-peak rose to 18–20 $\mu\text{g}/\text{m}^3$ from 5–6 $\mu\text{g}/\text{m}^3$; and proportion of PM₁ increased relative to coarser PM fractions (21–24% of PM₁₀ compared to 14% background). Eruption increased PM₁₀ and PM_{2.5} by ~50% in populated areas with low background concentrations, but its impact was not measurable in areas with high background sources. This suggests that ash-poor eruptions are one of, or the most, important source of PM₁ in Iceland, and potentially in other areas exposed to volcanic emissions.

55 There were significant fine-scale temporal (<1 hour) and spatial (<1 km) fluctuations in volcanic pollutant concentrations. In Reykjavík, two stations located <1 km of each other recorded peak hourly-mean concentrations of 480 and 250 $\mu\text{g}/\text{m}^3$ SO₂, and 5 and 0 exceedance events, respectively, within a ~12 hour plume advection event. This has implications for population exposures estimates.

1 Introduction

(Stewart et al., 2021) Globally, over a billion people are estimated to live within 100 km of an active volcano (Freire et al., 60 2019), a distance within which they might be exposed to volcanic air pollution (Stewart et al., 2021), and the number of potentially exposed people is growing because of building expansion into previously uninhabited areas near volcanoes. Basaltic fissure eruptions happen frequently near populated areas, for example at Kīlauea volcano on Hawaii (tens of episodes since 1983), Cumbre Vieja on La Palma 2021 and currently on Reykjanes, Iceland (from 2021 and ongoing at the time of writing). Even small, ash-poor fissure eruptions can cause severe air pollution episodes when they happen at the urban interface (Whitty et al., 2020).

65 Throughout this work, we will refer to ‘volcanic emissions’, and unless otherwise stated, our intended meaning is SO_2 -gas and PM (primary and secondary), collectively—Airborne volcanic emissions—commonly referred to as ‘volcanic air pollution’—pose both acute and chronic health hazards that can affect populations across large geographic areas (Stewart et al., 2021, and references within). Globally, over one billion people are estimated to live within 100 km of an active volcano (Freire et al., 2019), a distance within which they might be exposed to volcanic air pollution (Stewart et al., 2021). The number of potentially exposed people is growing, for example, due to building expansion into previously uninhabited areas near volcanoes. In this study, we examine the impacts of volcanic emissions on air quality in populated areas using high-resolution, high-quality observational data. We focus on the 2021 Fagradalsfjall fissure eruption on the Reykjanes Peninsula as a case study. Fissure eruptions are one of the most common types of volcanic activity that affects air quality. Recent examples of fissure eruptions at the urban interface include the Kīlauea volcano in Hawai‘i (with tens of episodes since 1983), Cumbre Vieja on La Palma in 2021, and the Reykjanes Peninsula in Iceland (11 eruptions since 2021). Fissure eruptions have low explosivity and produce negligible ash but release prodigious amounts of gases and aerosol particulate matter close to ground level. Even small fissure eruptions can cause severe air pollution episodes (Whitty et al., 2020).

(Apte and Manchanda, 2024)Fine-scale spatial variability in air pollutant concentrations—characterized by steep gradients over distances of just a few kilometres or less—is currently one of the most active areas of research within the broader field of air pollution (Apte and Manchanda, 2024). In urban areas, these fine-scale variations contribute to disparities in air quality, population exposure, and associated physical, mental, and social well-being (Apte and Manchanda, 2024, and references within). The 2021 Fagradalsfjall eruption provided a novel opportunity to investigate the fine-scale variability of volcanic air pollution in urban settings, as it was monitored by an exceptionally dense regulatory air quality network. (Apte and Manchanda, 2024)(Felton et al., 2019)Here, we use the term ‘regulatory’ to describe an air quality monitoring network operated by a national agency, employing certified commercial instrumentation with regulated setup and calibration protocols. These networks provide high-accuracy, high-precision measurements with high temporal resolution, but typically with low spatial resolution due to the high costs of installation (typically $> \text{€} 100,000$) and maintenance (typically $> \text{€} 100,000$ per annum). For example, Germany has approximately one regulatory station per $\sim 250,000$ people, with a similar density in the United States (Apte and Manchanda, 2024). In many volcanic regions, regulatory air quality monitoring is either absent or very sparse (Felton et al., 2019). Prior to our study, the best-observed case studies of volcanic air pollution came from Kīlauea volcano in Hawaii (in particular, its large fissure eruption in 2018), and the large Holuhraun fissure eruption 2014–2015 in Iceland (Crawford et al., 2021; Gíslason et al., 2015; Ilyinskaya et al., 2017; Schmidt et al., 2015; Whitty et al., 2020). These events were monitored by relatively few and distant regulatory stations—approximately 90 km from the eruption site at Holuhraun and about 40 km at Kīlauea. In contrast, the 2021 Fagradalsfjall eruption occurred in Iceland’s most densely populated region and in response, national authorities made a strategic decision early on to expand the regulatory network, ensuring that nearly every community was covered by at least one station. During the eruption, 27 regulatory stations were operational across Iceland, with 14 located within 40 km of the eruption site. Some stations were positioned less than 1 km apart, enabling unprecedented spatial resolution in observing volcanic air pollution.

Formatted: Font: Not Italic

Field Code Changed

(Apte and Manchanda, 2024; Sokhi et al., 2022) Regulatory air quality networks can be supplemented by so-called lower-cost sensors (LCS), which are typically small in size (a few centimetres) and cost approximately € 200. An active body of research on the expanding use of LCS highlights their potential to enhance the relatively sparse regulatory networks (reviewed in Apte and Manchanda, 2024; and Sokhi et al., 2022). For example, during a two-week campaign in 2018, the regulatory air quality network on Hawai'i Island was augmented with 16 LCS. This denser network significantly changed the estimates of population exposure to volcanic air pollution (Crawford et al., 2021). Despite their advantages in affordability and portability, LCS have notable limitations, including relatively poor accuracy and precision compared to regulatory-grade instruments, and a lack of standardised protocols for installation and maintenance. In our study, LCS were deployed to establish a rapid-response monitoring network directly at the eruption site, aimed at mitigating exposure hazards for the approximately 300,000 visitors who came to view the eruption. We present and discuss the use of LCS in a crisis mitigation context, which has broader relevance for other high-concentration, rapid-onset air pollution events, such as wildfires.

Formatted: Font: Not Italic

Formatted: Font: (Default) +Headings (Times New Roman)

110 1.1 Volcanic air pollutants and associated health impacts

Formatted: Heading 2, Outline numbered + Level: 2 + Numbering Style: 1, 2, 3, ... + Start at: 1 + Alignment: Left + Aligned at: 0 cm + Indent at: 0.63 cm

Much of the existing knowledge on the health impacts of volcanic air pollution comes from epidemiological and public health investigations of the eruptions at Holuhraun in Iceland and Kīlauea in Hawaii. The Holuhraun eruption was associated with increased healthcare utilisation for respiratory conditions in the country's capital area, located approximately 250 km from the eruption site (Carlsen et al., 2021a, b). These findings are consistent with observations from Kīlauea on Hawaii, which have been based on more qualitative health assessments and questionnaire-based surveys (Horwell et al., 2023; Longo, 2009; Longo et al., 2008; Tam et al., 2016). (Stewart et al., 2021) Volcanic emissions contain a wide array of chemical species, many of which are hazardous to human health (reviewed in Stewart et al., 2021). In this study, we focus on sulfur dioxide gas (SO_2) and three particulate matter (PM) size fractions— PM_{1} , $\text{PM}_{2.5}$, PM_{10} —which refer to particles with aerodynamic diameters less than 1 μm , 2.5 μm , and 10 μm , respectively. These pollutants are typically elevated both near the eruption source and at considerable distances downwind (Stewart et al., 2021). Throughout this work, we use the term 'volcanic emissions' to refer collectively to SO_2 and PM, unless otherwise specified.

Formatted: French (France)

Field Code Changed

Formatted: French (France)

Field Code Changed

Sulfur dioxide is abundant in volcanic emissions and a key air pollutant in volcanic areas (Crawford et al., 2021; Gíslason et al., 2015; Ilyinskaya et al., 2017; Schmidt et al., 2015; Whitty et al., 2020). Laboratory studies have shown that individuals with asthma are particularly sensitive to even relatively low concentrations of SO_2 (below 500 $\mu\text{g}/\text{m}^3$), and air quality thresholds are typically established to protect this vulnerable group (US EPA National Center for Environmental Assessment, 2008). Epidemiological studies in volcanic regions further indicate that children (defined as ≤ 4 years old) and the elderly (≥ 64 years old) are more susceptible to adverse health effects from above-threshold SO_2 exposure compared to the general adult population (Carlsen et al., 2021b). (Carlsen et al., 2021b) In recent decades, the number of regulatory air quality stations monitoring SO_2 has declined across much of the Global North, largely due to reductions in anthropogenic emissions, particularly from coal combustion. To our knowledge, Iceland currently maintains the highest number and spatial density of

Formatted: Font: Not Italic

Formatted: French (France)

Field Code Changed

Formatted: French (France)

regulatory SO₂ monitoring stations worldwide. This study therefore provides an unprecedented spatial resolution of SO₂ exposure in a densely populated, modern society affected by this pollutant.

Volcanic emissions are extremely rich in PM, comprising both primary particles emitted directly from the source and secondary particles formed through post-emission processes, such as sulfur gas-to-particle conversion. All three PM size fractions

135 reported in this study—PM₁, PM_{2.5}, PM₁₀—are known to be significantly elevated near volcanic sources. In fissure eruptions, PM₁ is typically the dominant size fraction (Ilyinskaya et al., 2012, 2017; Mather et al., 2003). (Brauer et al., 2024) has long been known to be (Janssen et al., 2013; McDonnell et al., 2000) (Gan et al., 2025; Guo et al., 2022; Yang et al., 2018; Zhang et al., 2020) (Tomášková et al., 2024) Exposure to PM air pollution, from natural and anthropogenic sources, has been linked to a wide range of adverse health outcomes, including cardiovascular and respiratory diseases, and lung cancer (Brauer et al., 2024, and references within). Health impacts have been observed even at low concentrations, with children and the elderly particularly vulnerable. The size of PM plays a critical role in determining health impacts. PM_{2.5} has long been associated with worse health outcomes compared to PM₁₀ (Janssen et al., 2013; McDonnell et al., 2000), and the importance of PM₁ is now a key focus in air pollution and health research. Multiple epidemiological studies from China have found PM₁ exposure to be more strongly correlated with negative health outcomes than PM_{2.5} (Gan et al., 2025; Guo et al., 2022; Yang et al., 2018; Zhang 140 et al., 2020). In Europe, epidemiological research on PM₁ health impacts is still in its early stages (Tomášková et al., 2024), largely due to a lack of high-quality observational data on PM₁ concentrations and exposure. This study contributes the first 145 regulatory-grade time series and exposure dataset of PM₁ from a volcanic source, as well as the first measurements of PM₁ in Iceland.

(Horwell, 2015; Tam et al., 2016) (Carlsen et al., 2021a) In volcanic emissions, concentrations of both SO₂ and PM in various 150 size fractions are consistently elevated, but their relative proportions vary depending on several factors, including distance from the source, plume age, and the rate of gas-to-particle conversion. Existing evidence suggests that this variability in plume composition may influence the associated health outcomes in distinct ways. An epidemiological study in Iceland comparing SO₂-dominated plumes with PM-dominated plumes found that the latter was associated with a greater increase in the dispensation of asthma medication and reported cases of respiratory infections (Carlsen et al., 2021a). In contrast, statistically 155 significant increases in healthcare utilization for chronic obstructive pulmonary disease (COPD) were observed only in association with exposure to SO₂-dominated plumes (Carlsen et al., 2021a).

Our study contributes a dataset on different types of volcanic air pollutants with a higher spatial resolution than has been previously been possible. This offers a foundation for future epidemiological research into the health impacts of recent and ongoing eruptions in Iceland.

160 1.2 Prior to this study, the best observed and studied impacts of volcanic emissions on air quality came from Kilauea in Hawaii (in particular the 2018 large fissure eruption), and Holuhraun large fissure eruption 2014–2015 in Iceland. Both of these volcanic sources degraded air quality at distances of hundreds of kilometres during times of activity (Crawford et al., 2021; Gíslason et al., 2015; Ilyinskaya et al., 2017; Schmidt et al., 2015; Whitty et al., 2020). A public health investigation of the Holuhraun eruption showed that it was associated with an increase in register-measured health care utilisation for respiratory

Formatted: Not Highlight

165 disease in Iceland's capital area 250 km from source (Carlsen et al., 2021a, b). The studies of Kīlauea and Holuhraun 2014–2015 eruptions were based on observations from relatively few and distal air quality stations; the closest reference-grade station to Holuhraun was at ~90 km distance, and ~40 km distance at Kīlauea. When the reference-grade air quality network on Hawaii was augmented by 16 low-cost SO₂- and PM_{2.5} sensors during a two-week campaign in 2018 it was shown that estimates of population exposure to volcanic air pollution can change significantly with a denser sensor network (Crawford et al., 2021).

170 Studies of volcanic plume chemistry in Holuhraun and Kīlauea eruptions have hypothesized that there may be significant fine-scale fluctuations in concentrations and dispersion patterns of volcanic gas and PM, potentially very close to the eruption site (Hlyinskaya et al., 2017, 2021), but this has not yet been observed in the field.

Fagradalsfjall 2021 was a small fissure eruption that happened in the most densely populated part of Iceland (~260,000 people or ~70% of the country's population lived within 40 km distance from the eruption site). The studies on Holuhraun 2014–2018 and Kīlauea 2018 eruptions made important discoveries about distal air quality impacts of large fissure eruptions (erupted volume >1 km³), which took place in relatively sparsely populated areas. Small eruptions (erupted volume from <0.1 up to 1 km³) are very important to investigate with regards to air pollution because they account for ~80% of eruptions worldwide (Siebert et al., 2015), and their impact on populated areas is likely to increase as the global population grows.

175 Fagradalsfjall 2021 presented a unique opportunity to advance our understanding of the intensity and dispersion patterns of volcanic air pollution in downwind populated areas. It was monitored by the densest reference-grade air quality monitoring network of any volcano in the world (to our knowledge) with 27 stations across Iceland, thereof 14 stations within 40 km distance from the eruption site. Some of these stations were located within 1 km from one another. This allowed our investigation into very fine-scale changes in spatial and temporal air quality impacts with respect to sulphur dioxide (SO₂), and different particulate matter size fractions (PM₁, PM_{2.5}, PM₁₀), which are the volcanic air pollutants that are likely to be

180 elevated, both at source and at significant distances downwind (Stewart et al., 2021).

185 This is also the first study reporting on a reference-grade timeseries of PM₁ during a volcanic eruption. PM₁ is known to be the dominant size fraction in volcanic emissions when measured directly at the volcanic source, but it has never been measured in downwind populated areas impacted by a volcanic eruption. Evidence-based air quality thresholds have been defined for SO₂, PM_{2.5} and PM₁₀ but not yet for PM₁, largely due to the paucity of reference-grade data on concentrations and dispersion

190 (World Health Organization, 2021). PM₁ is only recently being introduced in operational air quality monitoring worldwide (from 2020 in Iceland) and evidence-based guidelines for its levels are not yet established. Available studies unequivocally demonstrate a correlation between increased concentrations of PM₁ and negative health outcomes (Chen et al., 2017; Wang et al., 2011; Yang et al., 2018) and high-quality datasets on levels and variability of PM₁ are therefore important steps towards establishing air quality guidelines.

195 **1.1 Fagradalsfjall 2021 eruption description**

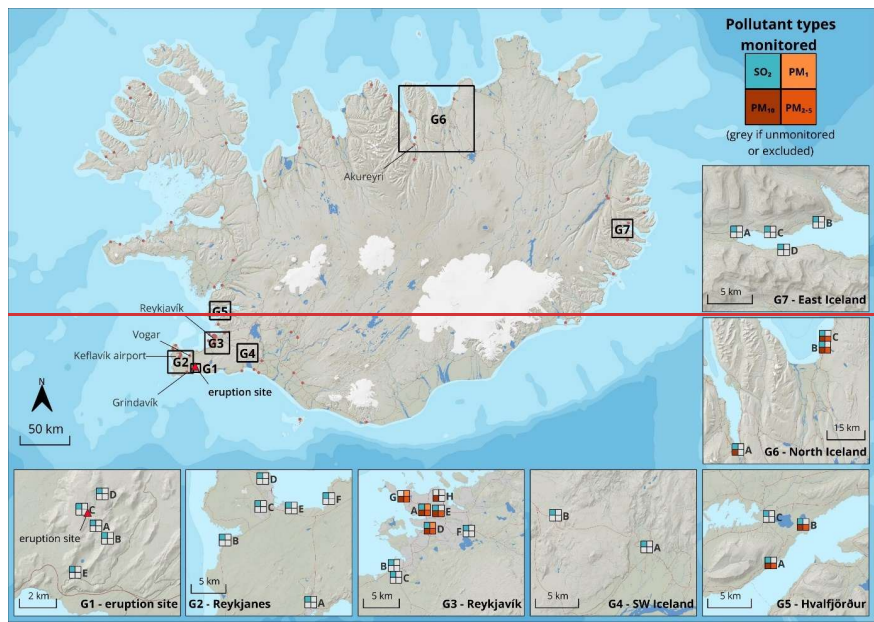
Fagradalsfjall 2021 (19 March – 19 September 2021) was the first eruption to happen in the most densely populated area of Iceland in ~800 years. The 2021 Fagradalsfjall eruption (19 March - 19 September 2021) was the first volcanic event on the

Reykjanes peninsula in nearly 800 years. This region is the most densely populated area of Iceland, with over 260,000 people—
200 around 70% of the national population—residing within 50 km of the eruption site. The eruption site was 9 km from the town
of Grindavík and approximately 25 km from the capital area of Reykjavík (Fig. 1). Although the eruption took place in an
uninhabited area, it attracted an estimated 300,000 visitors who observed the event at close range.

The eruption was a basaltic fissure eruption with an effusive and mildly explosive style, dominated by lava fountaining and
205 lava flows (Barsotti et al., 2023). While relatively small in size—emitting a total of ~0.3–0.9 Mt of SO₂ and covering an area
of 4.82 km² with lava (Barsotti et al., 2023; Pfeffer et al., 2024)—its proximity to urban areas and the high number of visitors
likely resulted in greater population exposure to volcanic air pollution than any previous eruption in Iceland.

210 and is considered to have been the beginning of a prolonged eruptive period on the Reykjanes peninsula, locally known as
Reykjanes Fires. At the time of writing, there have been 9 further eruptions on Reykjanes peninsula, thereof two in the
Fagradalsfjall volcanic system (August 2022 and July 2023), and seven in the adjacent Reykjanes-Svartsengi system
(December 2023–November 2024). Magma accumulation currently continues and based on the eruption history of the
215 Reykjanes peninsula, eruptive episodes activity may occur repeatedly for decades or centuries. Fagradalsfjall 2021 was a small
eruption (total ~0.3 to 0.9 Mt SO₂, 4.82 km² lava (Barsotti et al., 2023; Pfeffer et al., 2024)) but due to its location and
population growth it may have exposed more people to volcanic air pollution than any previous eruption in the country (Fig.
220 4). The eruption behaviour was very dynamic, and the number of active craters and the eruptive style changed several times
during its duration; for further details see (Barsotti et al., 2023). This eruption is considered to mark the onset of a new period
of frequent eruptions on the Reykjanes peninsula. Such periods, locally referred to as the ‘Reykjanes Fires’, have occurred
225 roughly every 1000 years, each lasting for decades to centuries. The last period of Reykjanes Fires ended with an eruption in
1240 CE (Sigurgeirsson and Einarsson, 2019). Since the 2021 eruption, ten further eruptions have occurred on the Reykjanes
peninsula: two within the Fagradalsfjall volcanic system (August 2022 and July 2023), and eight within the adjacent
Reykjanes-Svartsengi system (December 2023 to April 2025). Volcanic unrest continues at the time of writing, and based on
the eruption history of the Reykjanes peninsula, further eruptions may occur repeatedly over the coming decades or centuries.
The eruption site was at 9 km distance from the closest town of Grindavík; and over 70% of Iceland’s total population (263,000
out of 369,000 people) lived within 50 km distance, including the capital area of Reykjavík. The easily accessible site was also
visited by ~300,000 people for sightseeing during its course.

Formatted: English (United Kingdom)



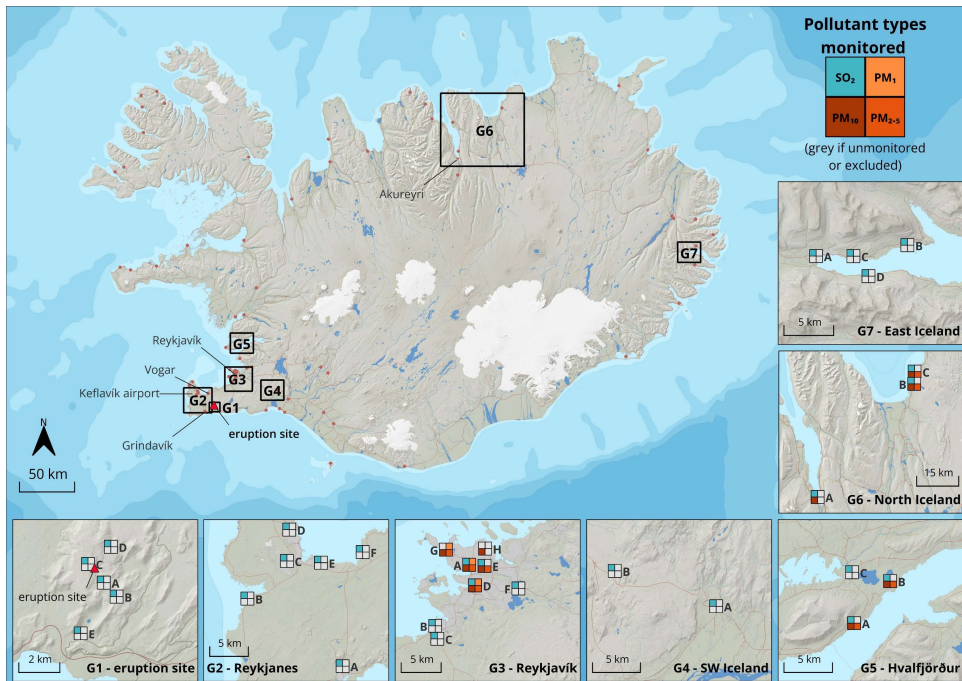


Figure 1: Map of Iceland showing the eruption site and air quality monitoring stations. The stations were organised in seven⁷ geographic clusters (each shown on the enlarged inserts). G1 - Eruption site (0-4 km distance from the volcanic venteruption site). G2 - Reykjanes peninsula (9-20 km distance). G3 - Reykjavik capital area (25-35 km distance). G4 - Southwest Iceland (45-55 km distance). G5 - Hvalfjörður (50-55 km distance). G6 - North Iceland (A and B ~280 km; C and D ~330 km distance). G7 - East Iceland (~400 km). The map shows the air pollutant species monitored at each station (SO₂, PM₁₀, PM_{2.5}, PM₁). Areas G2-G7 were monitored with reference-graderegulatory stations, while G1 had was monitored using lowerer-cost eruption response sensors. Source and copyright of basemap and cartographic elements: Icelandic Met Office & Icelandic Institute of Natural History.

230

2 Methods

Measurements Data were collected by two types of instrument networks:

1. A referencegraderegulatory municipal air quality (AQ) network, managed by the Environmental Agency of Iceland (EAI), which measured SO₂ and particulate matter (PM) in different size fractions.)
2. An and an eruption-response lower-cost sensor (gas-sensorLCS) -network measuring SO₂ only, operated by the Icelandic Meteorological Office (IMO, SO₂ only).

240

Formatted: List Paragraph, Numbered + Level: 1 + Numbering Style: 1, 2, 3, ... + Start at: 1 + Alignment: Left + Aligned at: 0.63 cm + Indent at: 1.27 cm

2.1 Reference-gradeRegulatory municipal network

The regulatory~~EAI~~ network monitors air quality across Iceland in accordance~~ing with~~ national legal mandates and complies with Icelandic Directive (ID) regulations. Most of the monitoring stations are located in populated areas and measure a variety of air pollutants. Here, we analysed SO₂ and PM in the PM₁, PM_{2.5}, and PM₁₀ size fractions, which are the most important 245 volcanic air pollutants with respect to human health in downwind populated areas (Stewart et al., 2021). Detection of SO₂ is based on pulsed fluorescence in the ultraviolet, and detection of PM is based on light scattering photometry and beta attenuation. The detection limits for the majority of the stations in this study were reported to be ~1-3 µg/m³ SO₂ and < 5 µg/m³ PM₁₀. Station-specific instrument details, detection and resolution limits, and operational durations are in Supplementary Table S1. Figure 1 shows the location of the stations and the air pollutants species measured thereat each site.

Formatted: Subscript

250 2.2 Eruption site sensors

At the eruption site (0.6-3 km from the active craters), the IMO installed a network of five commercially available lower-cost SO₂ LCS sensors between April and July 2021 to monitor air quality in the near-field. PM was not monitored with this network due to cost-benefit considerations as PM does not pose as acute a hazard as SO₂ for short-term exposure. -(The sensor 255 specifications and operational length-durations are detailed in Table S1). Figure 1 shows the location of those~~the~~ eruption-response SO₂ sensor networks. Stations A, B, and E were in close proximity to the public footpaths, while stations C and D were further afield to the north and northwest of the eruption site. The main purpose of the eruption-response network was to alert visitors when SO₂ levels were high rather than to provide accurate SO₂ concentrations. This was because lower-cost air quality sensors~~LCS~~ (gas and PM) are known to be significantly less accurate than reference-grade~~regulatory~~ instruments (Crilley et al., 2018; Whitty et al., 2022, 2020). Whitty et al. (2022) assessed the performance of lower-cost SO₂ LCS sensors 260 specifically in volcanic environments (same or comparable sensor models to the eruption site stations here~~those used here~~) and found that they were frequently subject to interferences restricting their capability to monitor SO₂ in low concentrations. The sensor accuracy limits identified in the field deployment study by~~of~~ (Whitty et al., (2022) were was significantly 265 poorer than the detection limits reported by the manufacturer. The sensors used in this study were not calibrated or co-located with higher-grade instruments during the field deployment as this network was, which seriously limits the accuracy of the obtained data~~-~~ set up ad hoc as part of an eruption crisis response by IMO. The crisis was two-fold: the eruption itself, and the 270 unprecedented crowding of people who wanted to view the eruption at very close quarters. The purpose of the sensor network was to alert visitors to high and potentially-hazardous concentrations, and it was not intended to produce a regulatory-grade dataset. Furthermore, the 2021 eruption occurred during national and international COVID-19 lockdowns, which reduced the opportunities for field-based research. Due to the low accuracy of the eruption site sensors, especially at lower concentration levels, we analysed the SO₂ data not quantitatively but as yes/no for exceeding the hourly-mean ID air quality threshold of 350 µg/m³. The lack of a field-based calibration of the sensors significantly limits the accuracy of the obtained LCS data, especially at lower concentration levels. For this reason we analysed the SO₂ data not quantitatively, but as a binary yes/no indicator for

Formatted: Subscript

Formatted: Not Highlight

Formatted: Font: Italic

275 exceeding the hourly-mean ID air quality threshold of $350 \mu\text{g}/\text{m}^3$. The threshold is ~ 2 orders of magnitude higher than the manufacturer-reported detection limits and therefore we consider it reasonable to assume that such concentrations would be detectable by the LCS.

2.3 Data processing

SO₂ measurements were downloaded from 24 ~~reference-grade regulatory~~ stations and 5 eruption site sensors, and PM₁₀, PM_{2.5} and PM₁ were downloaded from 12, 11 and 3 ~~reference-grade regulatory~~ stations, respectively. Data from ~~the reference-grade regulatory~~ stations were quality-checked and, where needed, re-calibrated by the EAI. Where the operational ~~length~~ duration was sufficiently long, we obtained SO₂ and PM measurements for both the eruption period and ~~the~~ non-eruptive background period.

280 We excluded from the analysis ~~any reference-grade regulatory~~ stations that had data missing for more than 4 months ($>70\%$) of the eruption period ($>70\%$). Further details on exclusion ~~reasons~~ of individual stations are in Table S1. ~~These~~ criteria excluded ~~both~~ PM₁₀ and PM_{2.5} from ~~2~~-two stations (G3-B, G3-C); and PM₁₀ from one station (G3-H). Data points that were 285 below instrument detection limits were set to $0 \mu\text{g}/\text{m}^3$ in our analysis. See Table S1 for ~~the~~ instrument detection limits of each instrument.

290 The eruption period was defined as 19 March/03/2021 20:00 – 19 September/09/2021 00:00 UTC in agreement with Barsotti et al., (2023). The background period was defined differently for SO₂ and PM. For SO₂, the background period was defined as 19/03/2020 00:00 - 19/03/2021 19:00 UTC, i.e. one full calendar year before the eruption. Outside of volcanic eruption periods, 295 SO₂ concentrations are generally low with little variability in the Icelandic atmosphere due to ~~the~~ absence of other sources, as shown by previous work (Carlsen et al., 2021a; Ilyinskaya et al., 2017), and subsequently confirmed by this study. The only exception is in the vicinity of aluminium smelters where relatively small pollution episodes occur periodically. A one-year long period was therefore considered as representative of the background SO₂ fluctuations. We checked our background dataset against a previously published comparable study in Iceland that used the same methods (Ilyinskaya et al., 2017) and found no 295 statistically significant difference.

PM background concentrations in Iceland are much higher and more variable than ~~those of~~ SO₂. PM frequently reaches high levels in urban and rural areas, ~~with and there are~~ significant seasonal variations (Carlsen and Thorsteinsson, 2021); the causes of this variability are discussed in the Results and Discussion. To account for this variability, we downloaded PM data for as many non-eruptive years as records existed, and analysed only the period 19 March 20:00 – 19 September 00:00 UTC in each 300 year, i.e. the period corresponding to the calendar dates ~~and months~~ of the 2021 eruption. From here on, we refer to this period as ‘annual period’. The annual periods in 2010, 2011, 2014, and 2015 were partially or entirely excluded from the non-eruptive background analysis due to eruptions in other Icelandic volcanic systems (Eyjafjallajökull 2010, Grímsvötn 2011, Holuhraun 2014-2015) and associated post-eruptive emissions and/or ash resuspension ~~events~~. The annual period of 2022, i.e. the year following the 2021 eruption, was partially included in the background analysis: measurements between 19 March 2022 and 1 305 August 2022 were included, but measurements from 2 August 2022 onwards were excluded because another eruptive episode

Formatted: Subscript

started in the Fagradalsfjall volcanic system on that date. Since August 2022 there have been nine⁸ more eruptions in the same area at intervals of weeks-to-months, and therefore we have not included more recent non-eruptive background data. Although the 2022 annual period is only partially complete, it was particularly important for statistical analysis of PM₁ as because operational measurements of this pollutant began only in 2020. The number of available background annual periods for PM₁₀ and PM_{2.5} varied depending on when each station was set up, between ranging from 1 and 12 stations with an average of 6 (Table S1).

We considered whether the year 2020 had lower PM₁₀ and PM_{2.5} PM and PM concentrations compared to other non-eruptive years because due to of COVID-19 pandemic societal restrictions and the extent to which this was likely to impact our results. The societal restrictions in Iceland were relatively light, for example, schools and nurseries remained opened throughout. We found that the average 2020 PM₁₀ and PM_{2.5} concentrations fell within the maximum-minimum range of the pre-pandemic years for all stations except at G3-E where PM₁₀ was 10% lower than minimum pre-pandemic annual average, and PM_{2.5} was 12% lower; and at G5-A where PM_{2.5} was 25% lower (no difference in PM₁₀). G3-E is at a major traffic junction in central Reykjavík, and G5-A is on a major commuter route to the capital area. For PM₁, only one⁴ station was already operational in 2020 (G3-A); PM₁ concentrations at this station were 20% higher in 2020 compared to 2022 (post-pandemic). We concluded that PM data from 2020 should be included in our analysis but we do point out note the potential impact of pandemic restrictions in the discussion where applicable.

2.4 Data analysis

We organised the air quality stations into geographic clusters to assess air quality by region. The geographic clusters were^{are} the immediate vicinity of the eruption site (G1, 0-4 km distance from the eruption site), the Reykjanes peninsula (G2, 9-20 km distance), the capital area of Reykjavík (G3, 25-35 km distance), Southwest Iceland (G4, 45-55 km distance), Hvalfjörður (G5, 50-55 km distance), North Iceland (G6-A ~280 km, G6-B and C ~330 km distance), and East Iceland (G7, ~400 km distance), (Fig. 1). Appendix A,B Figs. AB21-AB87 show SO₂ time-series data for each individual station in geographic clusters G1-G7, respectively. Appendix A,B Figs. AB98-,B9-,AB110 show PM time-series data for each individual station in geographic clusters G3, G5 and G6, respectively.

For each station that had data for both the eruption and background periods (SO₂ and PM), two-sample t-tests were applied to test whether the differences in background and eruption averages were statistically significant for the different pollutant species.

In addition to time series analysis, we analysed the frequency and number of events where pollutant concentrations exceeded air quality thresholds. Air quality thresholds are pollutant concentrations averaged over a set time period (usually 60 minutes or 24 hours), which are considered to be acceptable in terms of what is robustly known about the effects of the pollutant on health. An air quality threshold exceedance is an event where the pollutant concentration is higher than that set out in the threshold. Evidence-based air quality thresholds have been defined for SO₂, PM_{2.5} and PM₁₀, but not yet for PM₁, largely due

Formatted: Not Highlight

Formatted: Not Highlight

to the paucity of regulatory-grade data on concentrations, dispersion and exposure (World Health Organization, 2021). For 340 SO_2 , most countries, including Iceland, use an hourly-mean threshold of $350 \mu\text{g}/\text{m}^3$; and the threshold for total number of exceedances in a year is 24 (Icelandic Directive, 2016). We used these thresholds for SO_2 in our study. The air quality thresholds for PM are based on 24-hour averages, as there is currently insufficient evidence base for hourly-mean thresholds. For PM_{10} we used the Icelandic Directive (ID) and World Health Organisation (WHO) daily-mean threshold of $50 \mu\text{g}/\text{m}^3$, and for $\text{PM}_{2.5}$ we used the WHO daily-mean threshold of $15 \mu\text{g}/\text{m}^3$, as no ID threshold is defined. While there are currently no 345 evidence-based air quality thresholds available for PM_1 , some countries, including Iceland use selected values to help communicate the air pollutant concentrations and their trends to the public. The EAI uses a 'yellow' threshold for PM_1 at $13 \mu\text{g}/\text{m}^3$ when visualising data from the regulatory stations and this value was used here (termed 'EAI threshold').

For each station that had data for both the eruption and background periods (SO_2 and PM), two-sample t-tests were applied to 350 test whether the background and eruption averages were statistically significantly different for the different pollutant species. We then calculated the number of events where pollutant concentrations exceeded current air quality thresholds and guidelines. For SO_2 , we used the ID hourly-mean threshold of $350 \mu\text{g}/\text{m}^3$ used by the (Icelandic Directive, 2016). For PM_{10} we used the ID / World Health Organisation (WHO) daily-mean threshold of $50 \mu\text{g}/\text{m}^3$ (Icelandic Directive, 2016), and for $\text{PM}_{2.5}$ we used the WHO daily-mean threshold of $15 \mu\text{g}/\text{m}^3$ (World Health Organization, 2021), as no ID threshold is defined. There are 355 currently no evidence-based air quality thresholds available for PM_1 . However, the Environmental Agency of Iceland uses a 'yellow' threshold for PM_1 at $13 \mu\text{g}/\text{m}^3$ when visualising data from the reference-grade stations and this value was used here ('EAI threshold').

To be able to meaningfully compare the frequency of air quality threshold exceedance events for PM_{10} , $\text{PM}_{2.5}$ and PM_1 ($50, 360 15$ and $13 \mu\text{g}/\text{m}^3$, respectively) between the eruption and the non-eruptive background periods we normalised the number of exceedance events, as explained below. This was done because the eruption covered only one annual period (see the definition of 'annual period' in 2.3) but the number of available background annual periods varied between stations depending on how long they have been operational, ranging between 1 and 12 periods. We normalised by dividing the total number of exceedance events at a given station by the number of annual periods at the same station. For example, for a station where the non-eruptive background was 365 66 annual periods the total number of exceedance events was divided by 6 to give a normalised annual number of exceedance events. The eruption covered one annual period and therefore did not require dividing. We refer to this as 'normalised number of exceedance events' in the Results and Discussion. Table S1 contains summary statistics for all analysed pollutant means, maximum concentrations, number of air quality threshold exceedances, and number of background annual periods for PM data.

Three reference-grade regulatory stations within geographic cluster G3 (Reykjavík capital area) measured all three PM size 370 fractions (PM_1 , $\text{PM}_{2.5}$ and PM_{10}), which allowed us to calculate the relative contribution of different size fractions to the total PM concentration. Since PM size fractions are cumulative, in that PM_{10} contains all particles with diameters $\text{below} \leq 10 \mu\text{m}$, the size modes were subtracted from one another to determine the relative concentrations of particles in the following

Formatted: Not Highlight

Formatted: Not Highlight

Formatted: Subscript

Formatted: Subscript

Formatted: Not Highlight

375 categories: particles $\leq 1 \mu\text{m}$ in diameter, $1 - 2.5 \mu\text{m}$ in diameter and $2.5 - 10 \mu\text{m}$ in diameter. The comparison of size fractions between the eruption and the background was limited by the relatively short PM₁ time series and our results should be re-examined in the future when more non-eruptive measurements have been obtained.

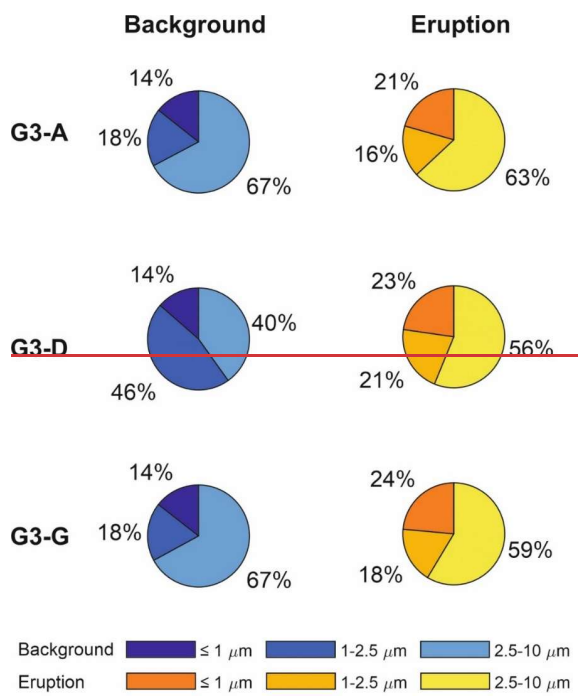
3 Results and discussion

3.1 Eruption-driven increase in PM₁ concentrations relative to PM₁₀ and PM_{2.5}

380 Emerging studies of the links between PM₁ and health impacts in urban air pollution have shown that even small increases in the PM₁ proportion within PM₁₀ can be associated with increasingly worse outcomes; e.g. liver cancer mortalities in China were found to increase for every 1% increase in the proportion of PM₁ within PM₁₀ (Gan et al., 2025). Time series of PM₁, PM_{2.5} and PM₁₀ concentrations were collected at three stations in Reykjavík capital (G3-A, G3-D and G3-G, Fig. 1), allowing us to compare the relative contributions of the three size fractions in this area (25–35 km distance from the eruption site). There was a measurable change during the eruption period compared to the background, with an increase in PM₁ mass proportion relative to PM₁₀ and PM_{2.5} at all 3 stations (Fig. 2). The proportion of PM₁ mass within PM₁₀ increased from 14–24% in the background (standard deviation 7–13%) to 24–24–32% during the eruption (standard deviation 16–19%); and within PM_{2.5} from 23–44% in the background to 52–57–60% during the eruption period within PM_{2.5}. The eruption-related change increase in proportion of the PM_{2.5} proportion within PM₁₀ was modest, not as clear, and varied considerably between the stations between 4% and 7% compared to the background. Two stations recorded a modest increase in PM_{2.5} relative to PM₁₀, from 32% background to 37–42% during the eruption period, but the third station recorded a decrease from 390 60% to 44%.

Formatted: Subscript

Formatted: Subscript



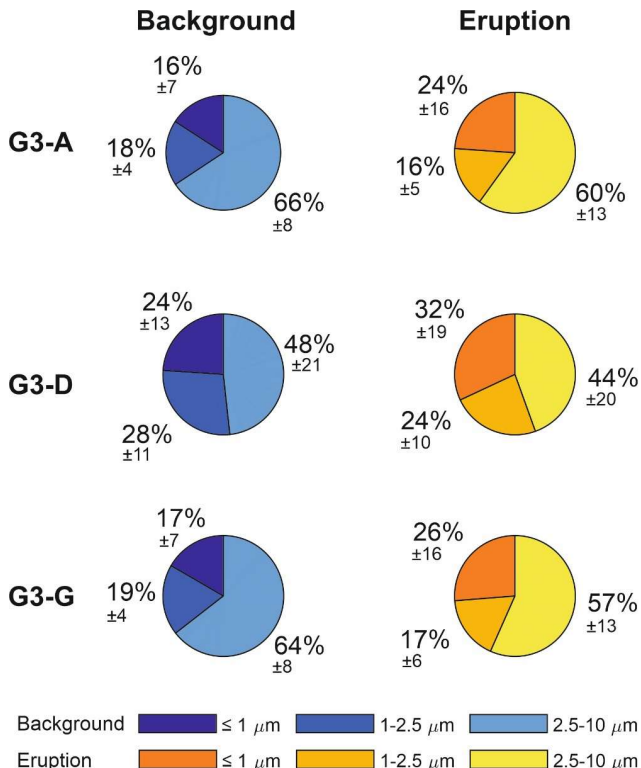


Figure 2: The relative contributions (in mass%) of three PM size fractions within PM_{10} (expressed as mass%) during the non-eruptive background and during the eruption. The size fractions shown are: PM $\leq 1 \mu\text{m}$, PM $1-2.5 \mu\text{m}$, and PM $2.5-10 \mu\text{m}$ in diameter. PM $\leq 1 \mu\text{m}$ in diameter, PM $1-2.5 \mu\text{m}$ in diameter and PM $2.5-10 \mu\text{m}$ in diameter. The %mass is shown as mean $\pm 1\sigma$ standard deviation. G3-A, G3-D and G3-E were the 3-stations in Iceland where all three size fractions were measured (all located within Reykjavik capital area).

This is a novel result. These are novel findings showing that volcanic plumes contribute a significantly higher proportion of PM_1 relative to both PM_{10} and $\text{PM}_{2.5}$ when sampled distally at a distal location from the source (25-35 km in this study). When sampled at the active vent, volcanic plumes from basaltic fissure eruptions have been previously been shown to contain a large amount of PM_1 , but also a substantial proportion of coarse PM ($> 2.5 \mu\text{m}$) (Ilyinskaya et al., 2017; Martin et al., 2011; Mason et al., 2021). At the vent, the composition of the fine and coarse size modes is typically very different with

the finer fraction is primarily formed via-through the conversion of SO₂ gas into sulphate particles, and-whereas the coarser fraction made-consists of fragmented silicate material (i.e. ash), which is-found in-some-may be present in small concentrations even in typically-ash-poor fissure eruptions (Ilyinskaya et al., 2021; Mason et al., 2021). The conversion of SO₂ gas to sulphate particles continues for hours to-and days after emission, generating new -from the volcanic vents forming new quantities of fine particles over time (Green et al., 2019; Pattantyus et al., 2018). In contrast, while-ash particles are not renewed-replenished in the plume after emission and are progressively lost-removed through deposition. This may-an explain 405 the elevated concentrations of particles in the finer size fractions observed downwind of the eruption site relative to the other coarser size fractions. This finding These findings have implications for public health hazards, as volcanic plumes most commonly affect populated areas located tens to hundreds of kilometres from the eruption site, has an implication for the health hazards posed by volcanic plumes in populated areas, which are typically located at a distance of tens-hundreds of kilometers from the eruption site. (Gan et al., 2025)

415

3.2 Significant but small increases in average pollutant levels

Most areas of Iceland, up to 400 km distance from the eruption site, recorded a small but statistically significant increase in average SO₂ and PM concentrations during the eruption compared to the background period.

Figure 3 and Table 1 compare-present SO₂ concentrations (hourly-means in $\mu\text{g}/\text{m}^3$), measured by reference-grade regulatory 420 stations across Iceland. During the non-eruptive background period, SO₂ concentrations were low (long term hourly-mean average of hourly-means generally $<2 \mu\text{g}/\text{m}^3$), which is in agreement with previous studies (Ilyinskaya et al., 2017). Stations in-the vicinity of near aluminium smelters (G5-1 and 2, G6-C, and G7-all) had higher long-term average values and periodically measured-recorded short-lived escalations in SO₂ hourly-mean concentrations of several tens-10s or 100s to hundreds of $\mu\text{g}/\text{m}^3$ 425 during the background period (Fig. 3, Table 1 and Table S1). Station G7-D (East Iceland at ~400 km distance from the eruption site) was the only one-station where the eruption-related increase in average SO₂ concentrations was below statistical significance. This station was in-a-vicinity-of-located near an aluminium smelter, and was also missing over 4/3-one-third of the eruption period data due to technical issues, which may have reduced the observed eruption impact.

The average SO₂ concentrations were higher during the eruption at all of-the reference-grade regulatory stations that had data 430 from both before and during the eruption ($n=16$), and the increase was statistically significant ($p<0.05$) at 15 out of the 16 stations. Across all seven-7 geographic clusters, the absolute increase in average SO₂ concentrations between the background and eruption period-was relatively low, on the order of a few $\mu\text{g}/\text{m}^3$ (Fig. 3 and Table 1). For example, the average concentration across the Reykjavík capital changed-increased from 0.32 $\mu\text{g}/\text{m}^3$ in the background to 4.1 $\mu\text{g}/\text{m}^3$ during the eruption.

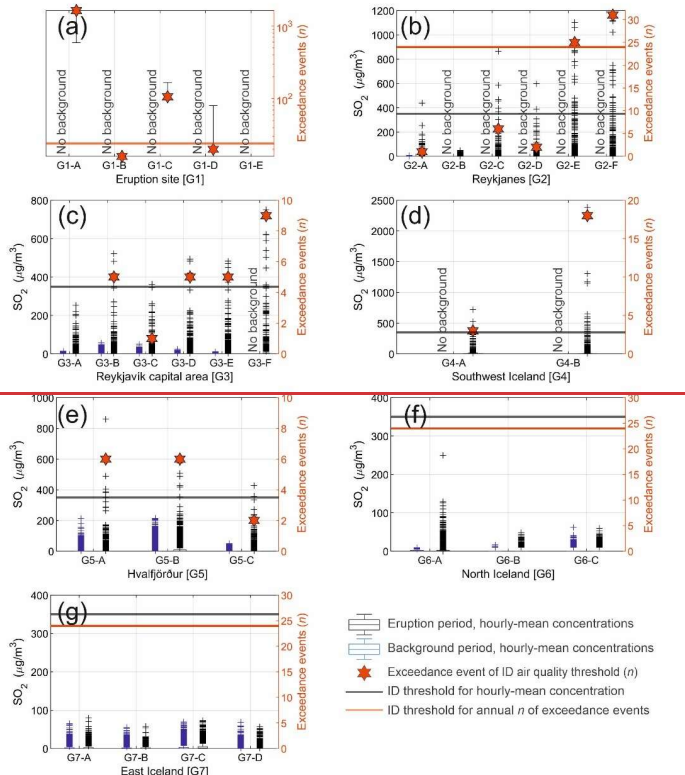
435 The absolute increases in average PM concentrations in all measured size fractions were relatively modest, similar to the
change observed in SO₂ average concentrations. Table 2 and Figs. 4-6 show PM₁₀, PM_{2.5} and PM₁ concentrations (daily means;
μg/m³) measured in the 3 geographic area where reference-grade monitoring was available. For example, in Reykjavík capital
(at stations where concentrations during the eruption period were statistically significantly higher than background), the
average PM₁₀ concentration changed from 9–10 μg/m³ in the background to 12–13 μg/m³ during the eruption period; average
440 PM_{2.5} from 3–4 μg/m³ background to ~5 μg/m³ eruption; and average PM₁ from 1.3–1.5 μg/m³ background to ~3 μg/m³ eruption
(Fig. 4).

445 **Table 1:** SO₂ concentrations (hourly-mean, $\mu\text{g}/\text{m}^3$) in populated areas around Iceland during both the non-eruptive background and during the Fagradalsfjall 2021 eruption. ‘Average’ is the long-term average hourly-mean of all stations within a geographic area \pm 1 σ standard deviation. ‘Peak’ is the maximum hourly-mean recorded by an individual station within the geographic area. ‘ID exceedances’: the number of times that the SO₂ concentrations exceeded the Icelandic Directive (ID) air quality threshold of 350 $\mu\text{g}/\text{m}^3$. The nNumber of AQ exceedances is the maximum number of exceedances recorded by an individual station within a geographic area.

Geographic area	N of stations	Distance from eruption site (km)	SO ₂ hourly-mean (µg/m ³)				ID exceedances (max n)	
			Background average ± standard deviation (1σ)	Eruption average ± standard deviation (1σ)	Background peak	Eruption peak	Background	Eruption
Reykjanes peninsula (G2)	6	9-20	0.13±0.45	4.8±44	7.7	2400	0	31
Reykjavik capital (G3)	6	25-35	0.32±1.8	4.1±21	57	750	0	9
South Iceland (G4)	2	45-55	No data	6.1±44	No data	2400	No data	18
Hvalfjörður (G5)	3	50-55	3.9±16	8.2±28	210	860	0	6
North Iceland (G6)	3	280-330	0.41±1.6	1.7±6.3	9.1 at 280 km; 62 at 330 km	250 at 280 km; 48 at 330 km	0	0

Geographic area	N of stations	Distance from eruption site (km)	SO ₂ hourly-mean (µg/m ³)				ID exceedances (max n)	
			Background average	Eruption average	Background peak	Eruption peak	Background	Eruption
Reykjanes peninsula (G2)	6	9-20	0.14	4.6	7.7	2400	0	31
Reykjavík capital (G3)	6	25-35	0.32	4.1	57	750	0	9
South Iceland (G4)	2	45-55	No data	6.1	No data	2400	No data	18
Hvalfjörður (G5)	3	50-55	3.8	8.2	210	860	0	6
North Iceland (G6)	3	280-330	0.38	1.7	9.1 at 280 km; 62 at 330 km	250 at 280 km; 48 at 330 km	0	0
East Iceland (G7)	4	400	1.8	2.4	69	79	0	0

450



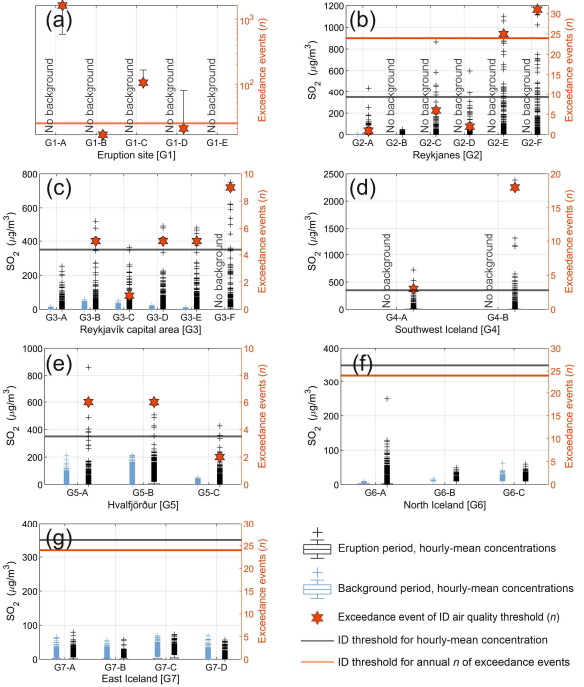


Figure 3: SO_2 hourly-mean concentrations ($\mu\text{g}/\text{m}^3$) and number of ID threshold exceedance events for SO_2 ($\mu\text{g}/\text{m}^3$), measured by 29 stations across seven geographical areas in Iceland (panels a-g). Pre-eruptive background data are shown for stations that were operational before the eruption began. The data are presented as box-and-whisker plots: boxes represent the interquartile range (IQR), the whiskers extend to $\pm 2.7\sigma$ from the mean, and crosses represent very high values (statistical outliers beyond $\pm 2.7\sigma$ from the mean). The data are shown as box-and-whiskers plots, with crosses representing extremely high values (statistical outliers). Note that the IQR is very low in most cases due to the negligible SO_2 concentrations in the clean local background; as a result, most of the SO_2 pollution episodes are statistical outliers. Pre-eruptive background is shown for stations that were in operation before the eruption started. Panel (a) shows eruption-site measurements collected by lower-accuracy sensors for which we only report number of exceedances of the ID air quality threshold ($350 \mu\text{g}/\text{m}^3$). Panels (b-g) show data from reference-grade stations in populated areas as SO_2 hourly-mean concentrations and the number of exceedance events. The ID air quality threshold of $350 \mu\text{g}/\text{m}^3$ (hourly-mean) is indicated by a black horizontal line in all panels. Red stars represent the number of times this threshold was exceeded at each station ("exceedance events"). The annual limit for cumulative hourly exceedance events is 24, shown by an orange horizontal line. Stations with red stars above the orange line exceeded the annual threshold. Panel (a) displays eruption-site measurements collected by LCS, for which only the number of exceedances of the ID air quality threshold ($350 \mu\text{g}/\text{m}^3$) is reported. Note the logarithmic scale used in panel (a). Panels (b-g) show data from regulatory stations in populated areas, including SO_2 hourly mean concentrations

Formatted: Subscript

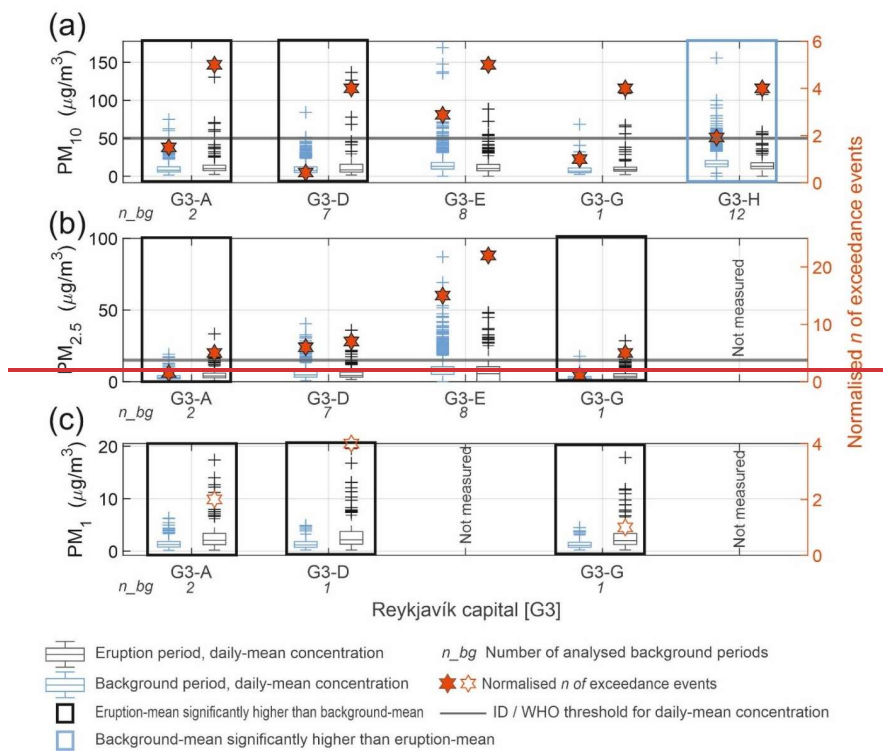
and the number of exceedance events. The 1D air quality threshold of $350 \mu\text{g}/\text{m}^3$ hourly mean is shown on all panels with a black horizontal line. The figure also shows whether the number of threshold exceedances at each station exceeded the recommended annual total ($n=24$, orange horizontal line). Note logarithmic scale for Eruption site (a). Time series plots for each station are available in Appendix A. Time series plots for each station are available in Appendix B Figures B1-B7.

Table 2 and Figs. 4-6 present PM_{10} , $\text{PM}_{2.5}$ and PM_1 concentrations (daily-means in $\mu\text{g}/\text{m}^3$) measured in the three geographic areas where regulatory-grade monitoring was available. Table 2 shows that when PM concentrations are averaged across all stations within a geographic area, there appears to be negligible or minimal change in average PM levels between the background and eruption periods. However, when individual stations are considered, small but statistically significant differences can be seen (Figs. 4-6), driven by fine-scale spatial variability in PM concentrations. During the eruption, average PM_1 concentrations were significantly higher at all monitored stations (Fig. 4). $\text{PM}_{2.5}$ and PM_{10} concentrations were also significantly higher at approximately half of the monitored stations (Figs. 4-6). At these stations, average PM_{10} concentrations increased from $9-10 \mu\text{g}/\text{m}^3$ during the background to $12-13 \mu\text{g}/\text{m}^3$ during the eruption; average $\text{PM}_{2.5}$ rose from $3-4 \mu\text{g}/\text{m}^3$ to $\sim 5 \mu\text{g}/\text{m}^3$; and average PM_1 increased from $1.3-1.5 \mu\text{g}/\text{m}^3$ to $\sim 3 \mu\text{g}/\text{m}^3$ (Fig. 4). Generally, PM_1 and $\text{PM}_{2.5}$ showed a more consistent eruption-related increase than PM_{10} , which agrees with our results on their relative proportions discussed in 3.1. During the eruption, PM_1 average concentrations were statistically-significantly higher at all monitored stations in Reykjavík capital (G3, Fig. 4). The $\text{PM}_{2.5}$ and PM_{10} concentrations were statistically-significantly higher during the eruption at approximately half of the monitored stations across all geographic stations (Figs. 4-6). The locations that recorded statistically significant eruption-related increases in average PM_{10} and $\text{PM}_{2.5}$ concentrations generally had lower non-eruptive background levels. The stations with higher background PM_{10} and $\text{PM}_{2.5}$ were generally situated near roads with heavy traffic. This suggests that local sources, such as road traffic, were more important sources of PM_{10} and $\text{PM}_{2.5}$ than the distal eruption. However, the eruption's impact on PM_{10} and $\text{PM}_{2.5}$ was more noticeable in areas with lower background concentrations. Average levels of PM_1 were unequivocally higher during the eruption period compared to the background, although this pollutant was only monitored in the Reykjavík capital area. It remains to be investigated whether volcanic contribution to PM_1 would also dominate over other sources in more distal communities.

Table 2 PM_{10} , $\text{PM}_{2.5}$ and PM_1 concentrations ($\mu\text{g}/\text{m}^3$, 24-h mean) in populated areas around Iceland during both the non-eruptive background ('B/G') and the Fagradalsfjall 2021 eruption ('Eruption'). 'Average' refers to the long-term mean of 24-hour values of all stations within a geographic area $\pm 1\sigma$ standard deviation. 'Peak' is the maximum 24 h-mean recorded by an individual station within the geographic area. 'AO exceedances' denotes the number of times PM concentrations exceeded the following thresholds: PM_{10} - $50 \mu\text{g}/\text{m}^3$; $\text{PM}_{2.5}$ - $15 \mu\text{g}/\text{m}^3$; PM_1 - $13 \mu\text{g}/\text{m}^3$. The 'AO exceedances' value is the maximum number of exceedances recorded by any single station within a geographic area.

Geographic area	n of stations (PM ₁₀ , PM _{2.5} , PM ₁)	PM ₁₀						PM _{2.5}						PM ₁						PM ₁₀								
		Average (24-h mean $\pm 1\sigma$, $\mu\text{g}/\text{m}^3$)			Peak (24-h mean, $\mu\text{g}/\text{m}^3$)			AQ exceedances (max n)			Average (24-h mean $\pm 1\sigma$, $\mu\text{g}/\text{m}^3$)			Peak (24-h mean, $\mu\text{g}/\text{m}^3$)			AQ exceedances (max n)			Average (24-h mean $\pm 1\sigma$, $\mu\text{g}/\text{m}^3$)			Peak (24-h mean, $\mu\text{g}/\text{m}^3$)			AQ exceedances (max n)		
		B/G	Eruption	B/G	Eruption	B/G	Eruption	B/G	Eruption	B/G	Eruption	B/G	Eruption	B/G	Eruption	B/G	Eruption	B/G	Eruption	B/G	Eruption	B/G	Eruption	B/G	Eruption	B/G	Eruption	B/G
Reykjavík capital (03)	5, 4, 3	25-35	15±11	14±14	170	140	2.9	5	6.6±6.8	5.7±6.2	87	48	15	22	1.4±0.94	2.8±2.6	6.3	20	0	4								
Hafnafjörður (05)	3	50-55	5.6±5.7	7.3±7.8	58	59	0.25	2	2.1±3.4	3.9±5.3	34	31	1	8														
North Iceland (06)	3	280-330	7.7±10	8.9±11	100	79	7.7	7	0.53±1.9	0.71±2.2	13	16	0	1														

Formatted: Normal



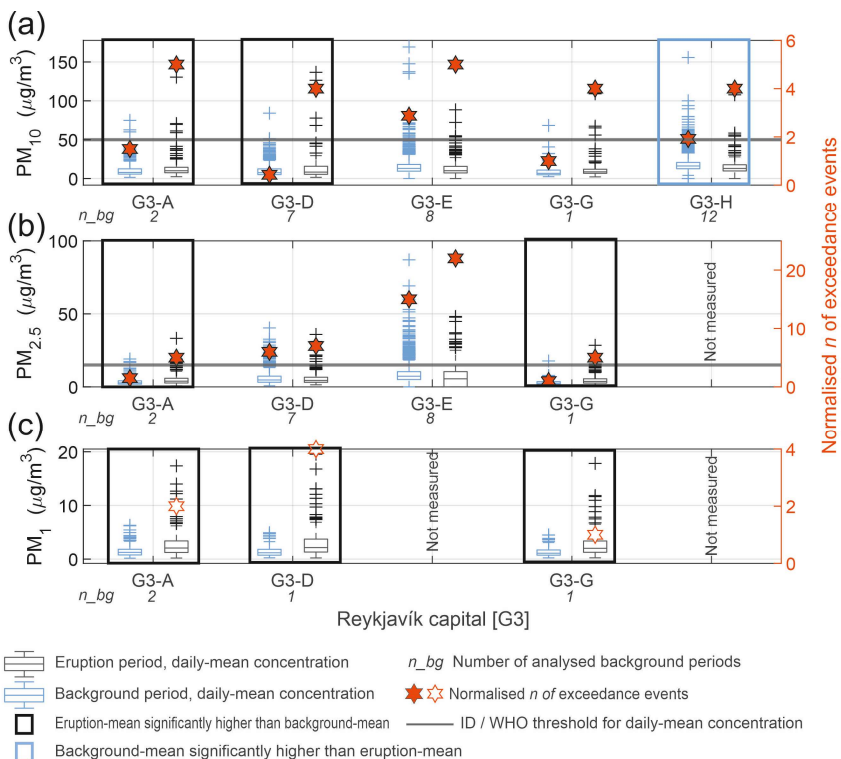
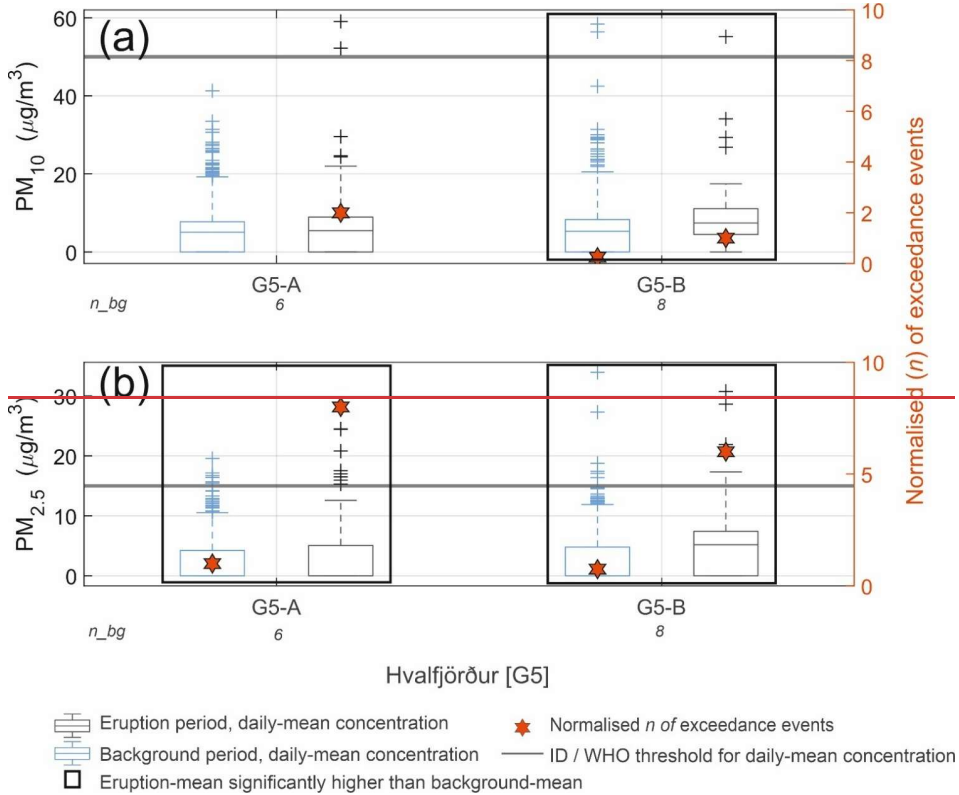


Figure 4: Daily-mean concentrations of (a) PM_{10} , (b) $\text{PM}_{2.5}$, and (c) PM_1 ($\mu\text{g}/\text{m}^3$), measured in the Reykjavík capital area. The data are presented as box-and-whisker plots, where boxes represent the interquartile range (IQR), the whiskers extend to $\pm 2.7\sigma$ from the mean, and crosses represent very high values (statistical outliers beyond $\pm 2.7\sigma$ from the mean). The median is shown with a horizontal line within each box. The concentrations are shown as box-and-whiskers plots, with crosses representing extremely high values (statistical outliers). Pre-eruptive background data are shown for stations which were in operation that were operational before the eruption started. The value, n_{bg} shown on the x-axis indicates the number of background annual periods available for each station (see Methods for the definition of a background annual period). Stations where the average concentration during the eruption period was statistically significantly higher ($p < 0.05$) than during the background are highlighted with a black box. Stations where the average concentration during the eruption period was statistically significantly lower than during the background are highlighted with a blue box. The absence of a

Formatted: Normal

box indicates no significant difference between the eruption and background periods. ~~S~~The figure-tars with solid orange fill represents shows the normalised number of times PM_{10} and $PM_{2.5}$ concentrations at each station exceeded the Icelandic Directive (ID) air quality thresholds of $50 \mu\text{g}/\text{m}^3$ and $15 \mu\text{g}/\text{m}^3$ ~~daily-mean~~^(24-hour mean), respectively. For PM_1 , ~~the figure~~ non-filled stars shows indicate the number of times the concentrations during the eruption exceeded the Environmental Agency of Iceland (EAI) threshold of $13 \mu\text{g}/\text{m}^3$ ~~(24-hour mean)~~^{daily-mean}. Different symbols (filled vs. non-filled stars) are used to distinguish between internationally accepted, evidence-based ID thresholds (PM_{10} and $PM_{2.5}$) and the locally applied EAI threshold for PM_1 , which is not internationally standardized. The number of threshold exceedance events is normalized to the length of the measurement period—refer to the main text for details on the normalization method. Time series plots for each station are available in Appendix A. The number of threshold exceedance events is normalized to the length of the measurement period—refer to the main text for an explanation of the method. Time series plots for each station are available in Appendix B Figure B8.



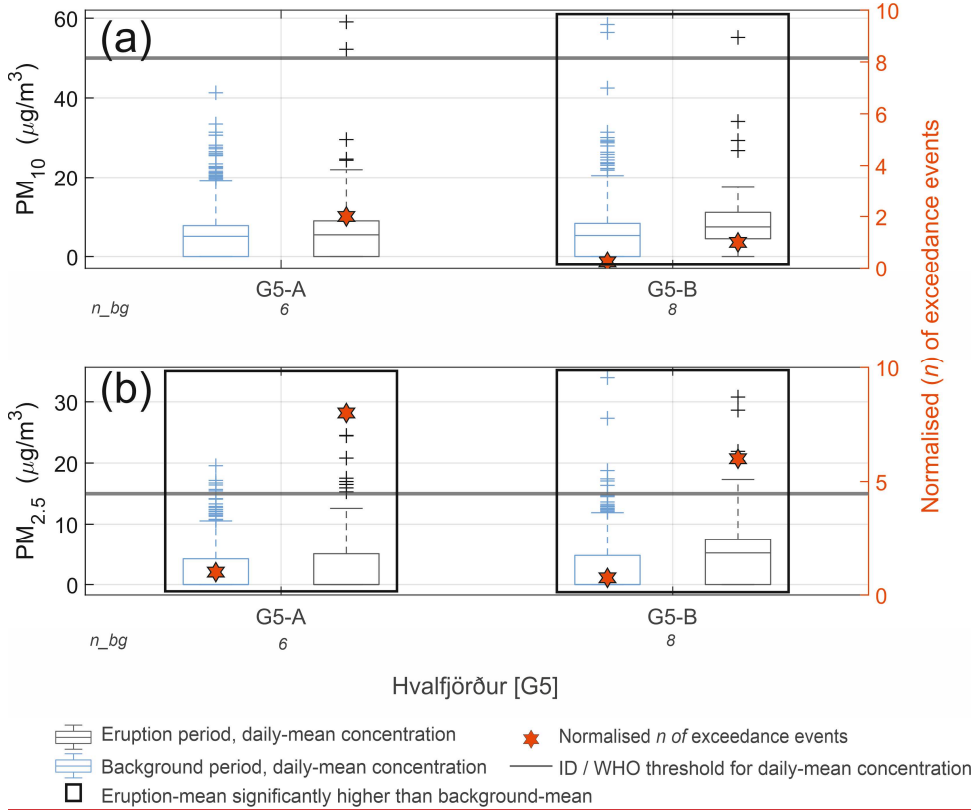
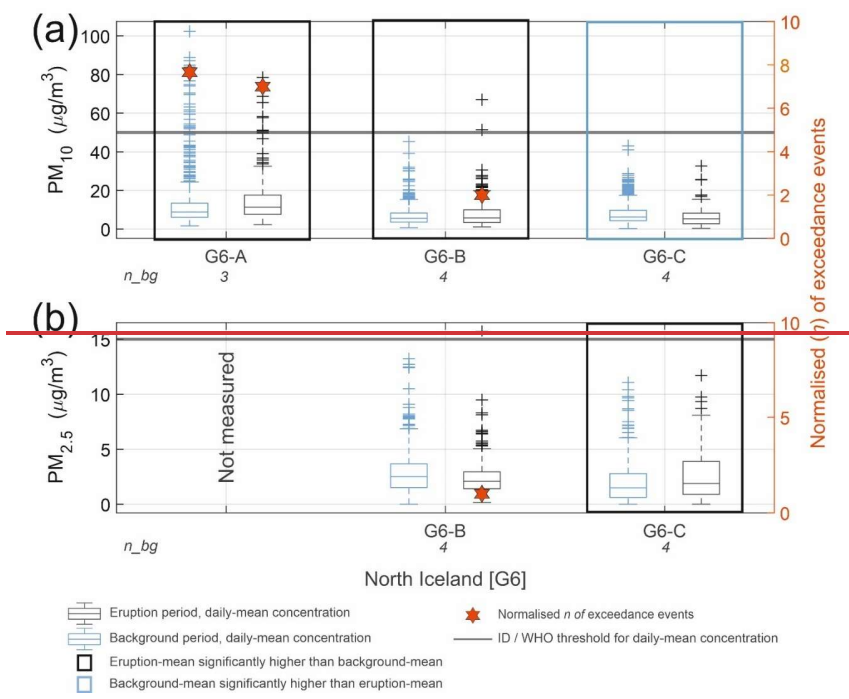
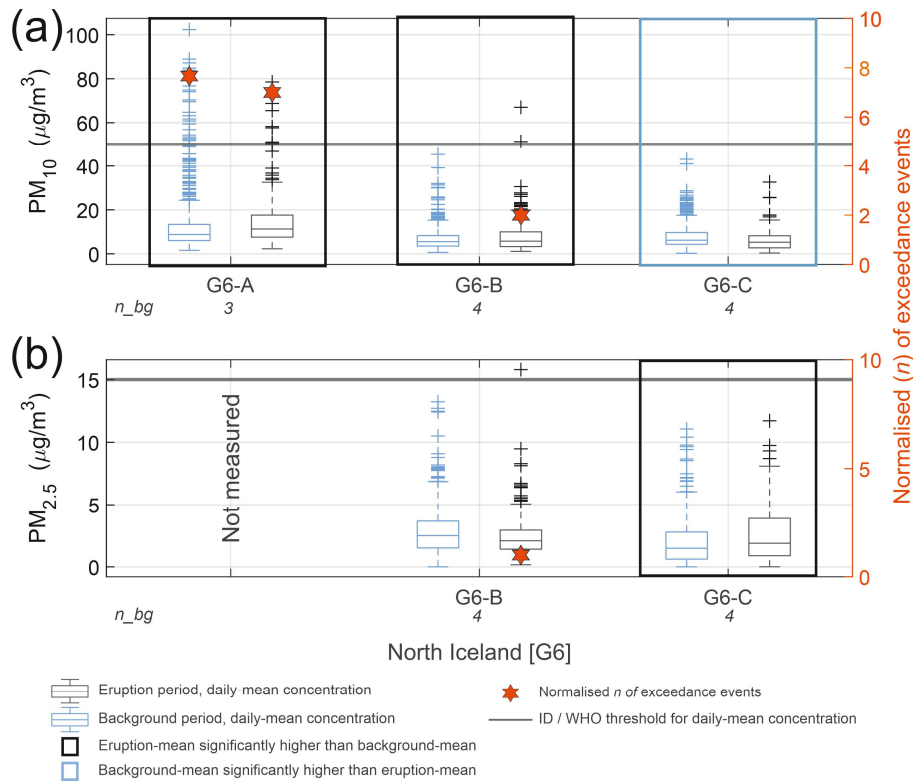


Figure 5: Daily-mean concentrations of (a) PM₁₀, and (b) PM_{2.5} ($\mu\text{g}/\text{m}^3$), measured in the Hvalfjörður area. The data are presented as box-and-whisker plots, where boxes represent the interquartile range (IQR), the whiskers extend to $\pm 2.7\sigma$ from the mean, and crosses represent very high values (statistical outliers beyond $\pm 2.7\sigma$ from the mean). The median is shown as a horizontal line within each box; if the median line is absent, the value is zero. Pre-eruptive background data are shown for stations that were operational before the eruption started. The value n_{bg} shown on the x-axis indicates the number of background annual periods available for each station (see Methods for the definition of a background annual period). Stations where the average concentration during the eruption period was significantly higher ($p < 0.05$) than during the background are highlighted with a black box. The absence of a box indicates no significant difference. Stars with solid orange fill show the normalized number of times PM₁₀ and PM_{2.5} concentrations at each station exceeded the Icelandic Directive (ID) air quality thresholds of 50 $\mu\text{g}/\text{m}^3$ and 15 $\mu\text{g}/\text{m}^3$ (24-hour mean), respectively. The number of threshold exceedance events is normalized to the length of the measurement period—refer to the main text for details on the normalization method. Time series plots for each station are available in Appendix A.

The concentrations are shown as box-and-whiskers plots, with crosses representing extremely high values (statistical outliers). Pre-eruptive background is shown for stations which were in operation before the eruption started, n_{bg} indicates the number of background annual periods for each station (see methods for definition of a background annual period). Stations where the average concentration during the eruption period was statistically significantly higher than the background are highlighted with a black box (absence of a box indicates no significant difference). The figure shows the normalised number of times PM_{10} and $PM_{2.5}$ concentrations at each station exceeded the ID air quality threshold of 50 and 15 $\mu\text{g}/\text{m}^3$ daily-mean, respectively. The number of threshold exceedance events is normalised to the length of the measurement period – refer to the main text for an explanation of the method. Time series plots for each station are available in Appendix B Figure B9.





550 **Figure 6: Daily-mean concentrations of (a) PM_{10} , and (b) $PM_{2.5}$ ($\mu g/m^3$), measured in North Iceland.** The concentrations are shown as box-and-whisker plots, with crosses representing extremely high values (statistical outliers). Pre-eruptive background is shown for stations which were in operation before the eruption started. n_{bg} indicates the number of background annual periods for each station (see methods for definition of a background annual period). Stations where the average concentration during the eruption period was significantly higher than the background are highlighted with a blue box. Absence of a box indicates no significant difference between eruption and background. The figure shows the normalised number of times PM_{10} and $PM_{2.5}$ concentrations at each station exceeded the ID air-quality threshold of 50 and 15 $\mu g/m^3$ daily-mean, respectively. The number of threshold exceedance events is normalised to the length of the measurement period – refer to the main text for an explanation of the method. Time series plots for each station are available in Appendix Daily-mean concentrations of (a) PM_{10} , and (b) $PM_{2.5}$ ($\mu g/m^3$), measured in North Iceland. The data are presented as box-and-whisker plots, where boxes represent the interquartile range (IOR), the whiskers extend to $\pm 2.7\sigma$ from the mean, and crosses represent very high values (statistical outliers beyond $\pm 2.7\sigma$ from the mean). The median is shown as a horizontal line within each box; if the median line is absent, the value is zero. Pre-eruptive background data are shown for stations that were operational before the eruption started. The value n_{bg} shown on the x-axis indicates the number of background annual periods available for each station (see Methods for the definition of a background annual

555

560

period). Stations where the average concentration during the eruption period was significantly higher ($p < 0.05$) than during the background are highlighted with a black box. Stations where the average concentration during the eruption was significantly lower than during the background are highlighted with a blue box. The absence of a box indicates no significant difference. Stars with solid orange fill show the normalized number of times PM_{10} and $PM_{2.5}$ concentrations at each station exceeded the Icelandic Directive (ID) air quality thresholds of $50 \mu\text{g}/\text{m}^3$ and $15 \mu\text{g}/\text{m}^3$ (24-hour mean), respectively. The number of threshold exceedance events is normalized to the length of the measurement period—refer to the main text for details on the normalization method. Time series plots for each station are available in Appendix A.

565

570 **B-Figure B10.**

Table 2 PM₁₀, PM_{2.5} and PM₁-concentrations ($\mu\text{g}/\text{m}^3$, 24-h mean) in populated areas around Iceland during the non-eruptive background ('B/G') and during the Fagradalsfjall 2021 eruption ('Eruption'). 'Average' is the average 24-h mean of all stations within the geographic area. 'Peak' is the maximum 24-h mean recorded by an individual station within a geographic area. 'AQ exceedances' is number of times that the PM-concentrations exceeded the following concentrations: PM₁₀-50 $\mu\text{g}/\text{m}^3$ 24-h mean; PM_{2.5}-15 $\mu\text{g}/\text{m}^3$ 24-h mean; PM₁-13 $\mu\text{g}/\text{m}^3$ 24h mean. 'AQ exceedances' is the maximum number of exceedances recorded by an individual station within a geographic area.

Geographic area	n of stations (PM ₁₀ , PM _{2.5} , PM ₁)	Distance from eruption site (km)	PM ₁₀				PM _{2.5}				PM ₁									
			Average (24-h mean in $\mu\text{g}/\text{m}^3$)		Peak (24-h mean in $\mu\text{g}/\text{m}^3$)		AQ exceedances (max n)		Average ($\mu\text{g}/\text{m}^3$)		Peak (24-h mean in $\mu\text{g}/\text{m}^3$)		AQ exceedances (max n)		Average (24-h mean in $\mu\text{g}/\text{m}^3$)		Peak (24-h mean in $\mu\text{g}/\text{m}^3$)		AQ exceedances (max n)	
			B/G	Eruption	B/G	Eruption	B/G	Eruption	B/G	Eruption	B/G	Eruption	B/G	Eruption	B/G	Eruption	B/G	Eruption		
Reykjavík capital (G3)	5, 4, 3	25-35	11	13	170	140	2.9	5	4.6	5.3	87	48	15	22	1.4	2.8	6.3	20	0	4
Hvalfjörður (G5)	3	50-55	5.7	7.6	58	59	0.25	2	2.1	4.2	34	31	1	8	No data					
North Iceland (G6)	3	280-330	8.1	8.6	100	79	7.7	7	0.53	0.72	13	16	0	1	No data					

Generally, PM₁ and PM_{2.5} showed a more consistent eruption-related increase than PM₁₀, which agrees with our results on their relative proportions discussed in 3.1. During the eruption, PM₁ average concentrations were statistically significantly higher at all monitored stations in Reykjavík capital (G3, Fig. 4). The PM_{2.5} and PM₁₀ concentrations were statistically significantly higher during the eruption at approximately half of the monitored stations across all geographic stations (Figs. 4-6). The locations that recorded significant eruption related increases in average PM₁₀ and PM_{2.5} concentrations generally had lower non-eruptive background concentrations. The stations with higher background PM₁₀ and PM_{2.5} were generally located closer to roads with heavy traffic; this shows that local sources such as road traffic were more important PM₁₀ and PM_{2.5} pollution sources than the distal eruption, but the eruption impacts on average levels of PM₁₀ and PM_{2.5} were more noticeable in areas with lower background concentrations. Average levels of PM₁ were unequivocally higher during the eruption period compared to the background, but this pollutant was only monitored in the Reykjavík capital area. It remains to be investigated whether volcanic contribution to PM₁ would also dominate over other sources in more distal communities.

3.3 Impact on pollutant peak concentrations and number of air quality exceedance events

Unlike the modest (or, at some stations, negligible) increases in the average concentrations of PM and SO₂, the eruption was associated with large increases in the number of air quality threshold exceedance events in the near- and far-field. Unlike the modest—or in some cases negligible—increases in average concentrations of PM and SO₂, the eruption was associated with substantial increases in the number of air quality threshold exceedance events in both near-field and far-field locations.

Figure 3 and Table 1 compare the background and the eruption periods with respect to peak concentrations, and the number of Iceland Directive (ID) threshold exceedance events for SO₂ (350 µg/m³ hourly-mean). During the non-eruptive background the SO₂ concentrations never exceeded the ID threshold at any of the stations. During the eruption, the numbers of threshold exceedance events ranged between 0 and 31 at individual stations and were, broadly speaking, the highest closer to the eruption site (Fig. 3 and Table 1). Figure 3 and Table 1 compare the background and eruption periods in terms of peak SO₂ concentrations and the number of exceedance events relative to the Icelandic Directive (ID) air quality threshold of 350 µg/m³ (hourly-mean). During the non-eruptive background period, SO₂ concentrations did not exceed the ID threshold at any station. In contrast, during the eruption, the number of exceedance events ranged from 0 to 31 at individual stations, and were, in broad terms, highest closer to the eruption site (Fig. 3 and Table 1). The ID threshold for total annual hourly-mean exceedances (*n* = 24) was exceeded in the geographic cluster immediately adjacent to the eruption site (G1), where up to 1,600 exceedance events were recorded at an individual station. Additionally, two communities on the Reykjanes Peninsula (G2) recorded 25 and 31 exceedance events, respectively. However, there were noticeable fine-scale spatial variations in SO₂ concentrations within individual geographical areas as discussed further in 3.4. The ID threshold for total annual hourly-mean exceedances (*n* = 24) was exceeded in the geographic cluster in the immediate vicinity of the eruption site (G1; up to 1600 events at an individual station), and in two communities on the Reykjanes peninsula (G2; 25 and 31 events, respectively). We attributed the combination of a relatively low absolute increase in the average SO₂ concentrations, and a large increase in peak

Formatted: Font: Italic

615 concentrations to a combination of the pulsating behaviour of the eruption emissions, and highly variable local meteorological conditions (wind rose for eruption site is in Appendix B Fig. B11 (Barsotti et al., 2023; Pfeffer et al., 2024)). This meant that the volcanic plume was only periodically advected into individual populated areas, rather than being a persistent source of pollution in the same location. We attribute the combination of a relatively low absolute increase in average SO₂ concentrations and a large increase in peak concentrations to a combination of the dynamic nature of the eruption emissions (Barsotti et al., 2023; Pfeffer et al., 2024) and highly variable local meteorological conditions (wind rose for the eruption site in Fig. 620 A12) (Barsotti et al., 2023; Pfeffer et al., 2024)). These factors resulted in the volcanic plume being intermittently advected into populated areas, rather than acting as a continuous source of pollution.

625 PM₁ concentrations never exceeded the EAI threshold (13 µg/m³) in the background period but during the eruption exceeded between 3 and 5 times at all stations where it was monitored (Fig. 4, Table 2). The number of PM₁₀ and PM_{2.5} exceedance events was higher during the eruption period at all stations in Reykjavík capital area (G3) and in Hvalfjörður (G5), and at 2 out of 3 North Iceland (G6) stations that recorded any threshold exceedances. PM₁ concentrations did not exceed the EAI threshold of 13 µg/m³ during the background period. However, during the eruption, exceedances occurred between three and five times at all stations where PM₁ was monitored (Fig. 4, Table 2). The number of PM₁₀ and PM_{2.5} exceedance events was also higher during the eruption period at all stations in the Reykjavík capital area (G3) and in Hvalfjörður (G5), as well as at two out of three stations in North Iceland (G6) that recorded any threshold exceedances.

630 PM₁ peak concentrations increased from 5–6 µg/m³ peak daily-mean during the background period to ~20 µg/m³ peak daily-mean during the eruption period, across all 3 monitored stations in Reykjavík capital (G3). Volcanic impact on PM₁₀ and PM_{2.5} was more variable compared to PM₁. Peak PM₁ concentrations (daily-mean) increased from 5–6 µg/m³ during the background period to approximately 20 µg/m³ during the eruption period across all three monitoring stations in the Reykjavík capital area (G3). The volcanic impact on PM₁₀ and PM_{2.5} was more variable. Stations in the Reykjavík capital area stations with cleaner PM₁₀ and PM_{2.5} backgrounds (defined here as peak daily-mean below <80 µg/m³ for PM₁₀ and below <20 µg/m³ for PM_{2.5}) 635 showed larger eruption-related impacts from the eruption than stations with more polluted background conditions (peak daily-means \geq 110 µg/m³ for PM₁₀ and \geq 40 µg/m³ for PM_{2.5}). At the cleaner stations, peak daily-mean concentrations increased by up to 40–60 µg/m³ for PM₁₀ and by 10–14 µg/m³ for PM_{2.5} during the eruption. In contrast, the more polluted stations did not 640 exhibit noticeable increases in peak PM₁₀ or PM_{2.5} concentrations. The cleaner stations show eruption-related increases of up to 40–60 µg/m³ PM₁₀ and 10–14 µg/m³ PM_{2.5} above peak background levels while the more polluted stations did not have noticeable increases in peak daily-means of PM₁₀ and PM_{2.5} during the eruption. Further afield, in Hvalfjörður and North Iceland (Figs. 5–6), the number of monitoring stations was too low for a statistical analysis, but generally the same pattern was 645 observed: stations with lower non-eruptive background PM₁₀ and PM_{2.5} generally recorded increases in peak daily-mean concentrations of up to ~20 and 5 µg/m³, respectively, above background levels. Further afield, in Hvalfjörður and North Iceland (Figures 5–6), the number of monitoring stations was too low for statistical analysis. However, a similar pattern was

Formatted: Subscript

observed: stations with lower non-eruptive background PM_{10} and $PM_{2.5}$ levels generally recorded increases in peak daily mean concentrations of up to $\sim 20 \mu\text{g}/\text{m}^3$ and $\sim 5 \mu\text{g}/\text{m}^3$, respectively, above background levels.

650 The statistically significant impact on average and peak PM levels observed in the Reykjavík capital and further afield (in up to at least 300 km distance) is remarkable considering the relatively small size of the eruption and the importance of non-volcanic PM sources in Iceland. In rural areas, the main non-volcanic source of PM is re-suspended natural dust sourced from highland deserts (Butwin et al., 2019), with higher levels in the drier summer seasons. In urban areas, the non-volcanic PM pollution peaks are typically higher in the winter with the main source being tarmac road erosion by studded tyres (Carlsen and Thorsteinsson, 2021). The statistically significant impact on both average and peak PM levels observed in the Reykjavík capital area and as far as 300 km from the eruption site is remarkable, given the relatively small size of the eruption and the prominence of non-volcanic PM sources in Iceland. In rural regions, the primary non-volcanic source of PM is resuspended natural dust from highland deserts, with elevated levels typically occurring during the drier summer months (Butwin et al., 2019). In urban areas, non-volcanic PM pollution peaks are generally higher in winter, primarily due to tarmac erosion caused by studded tyres (Carlsen and Thorsteinsson, 2021). The unequivocal eruption-related increase in average and peak 660 concentrations of PM_1 suggests that volcanic fissure eruptions are one of, or potentially the most, important source of PM_1 in Iceland, at least during the summer months. Table 3 compares concentration ratios of the three measured PM size fractions in Reykjavík across three scenarios: a representative eruption-free background period, the 2021 volcanic plume, and two Icelandic desert dust storms in 2023. Our analysis is based only on summer conditions because of the timing of the 2021 665 eruption. During winter, contributions from tarmac erosion due to studded tyres may influence these ratios, and short-lived peak concentrations may also occur during New Year's Eve fireworks. Data from winter-time eruptions are needed to better understand seasonal variability in PM_1 source contributions.

670 Although based on a limited dataset, our comparison suggests distinct 'fingerprint' ratios for the different pollution sources (Table 3), between a representative eruption-free background; the 2021 volcanic plume; and two Icelandic desert dust storms in 2023. The comparison is made based on a small dataset but suggests distinct 'fingerprint' ratios for the different pollution sources. These ratios may be used for identifying sources of PM pollution episodes in Reykjavík and potentially other distal populated areas, especially when the sources are difficult to identify using meteorological and/or visual observations. During the winter months, the contribution of tarmac erosion by studded tyres may affect the ratios; and higher short-lived peak concentrations may happen during New Years Eve fireworks—more data on winter-time eruptions is needed to establish this. These ratios may be useful for identifying the sources of PM pollution episodes in Reykjavík and potentially in other distal 675 populated areas, especially when source attribution is challenging using meteorological or visual observations. -

Table 3. Concentration ratios of PM size fractions (hourly-means, $\mu\text{g}/\text{m}^3$) associated with different pollution sources in Reykjavík capital area. Green-coloured rows show ratios during periods considered to be representative of typical Reykjavík background: ‘Summer period’ when studded tyres are not in use (banned between 14 April and 31 October), and a period during the 2021 eruption when the plume was being advected away from Reykjavík. Concentration ratios of PM size fractions (hourly-means, $\mu\text{g}/\text{m}^3$) associated with different pollution sources in the Reykjavík capital area. Rows 1 and 2 represent periods considered typical of Reykjavík background conditions: the ‘Summer period’, when studded tyres are not in use (banned between April and November), and a period during the 2021 eruption when the volcanic plume was advected away from Reykjavík. Orange-coloured rows show ratios during the 2021 eruption when the plume was advected to Reykjavík; for definitions of fresh and mature plume see section 3.4. ‘Desert dust’ are pollution episodes caused by Icelandic highland desert storms (source area ~200 km from Reykjavík), confirmed by IMO meteorological and visual observations. Station G3-G is listed first as it is considered to be the most sensitive one to the presence of volcanic plume due to low background concentrations from local sources. Rows 3–6 show ratios during the 2021 eruption when the plume was advected toward Reykjavík. For definitions of ‘fresh’ and ‘mature’ plume, see Section 3.4. Rows 7 and 8, labelled ‘Desert dust’, correspond to pollution episodes caused by Icelandic highland desert storms (source area ~200 km from Reykjavík), confirmed by meteorological and visual observations from the Icelandic Meteorological Office (IMO). Station G3-G is listed first, as it is considered the most sensitive to the presence of volcanic plume due to its low background concentrations from local sources.

	Start date	Start time	End date	End time	G3-G			G3-A			G3-D			G3-G			G3-A			G3-D		
					PM ₁ /PM ₁₀	PM ₂ /PM ₁₀	PM ₄ /PM ₁₀	PM ₂ /PM _{2.5}	PM ₁ /PM _{2.5}	PM ₄ /PM _{2.5}	PM _{2.5} /PM ₁₀											
Summer period, no eruption	01/05/2020	00:00	01/09/2020	00:00	0.16	0.15	0.13	0.44	0.43	0.22	0.35	0.34	0.61									
Eruption but no plume in Reykjavík	01/04/2021	09:00	02/04/2021	10:00	0.17	0.19	0.24	0.41	0.43	0.45	0.42	0.43	0.54									
Fresh plume	18/07/2021	10:00	19/07/2021	16:00	0.65	0.68	0.7	0.9	0.92	0.84	0.72	0.73	0.78									
Mature plume 1	28/04/2021	08:00	29/04/2021	20:00	0.43	0.29	0.49	0.8	0.73	0.8	0.53	0.39	0.6									
Mature plume 2	19/05/2021	14:00	21/05/2021	11:00	0.71	0.65	0.85	0.96	0.95	0.95	0.73	0.68	0.89									
Mature plume 3	01/07/2021	09:00	06/07/2021	08:00	0.67	0.59	0.65	0.91	0.88	0.84	0.74	0.66	0.74									
Desert dust 1	03/11/2023	13:00	04/11/2023	02:00	0.02	n/a	0.02	0.11	n/a	0.13	0.15	n/a	0.15									
Desert dust 2	08/11/2023	14:00	09/11/2023	00:00	0.01	n/a	0.01	0.1	n/a	0.086	0.15	n/a	0.15									

680

685

690

695

3.4 Fine-scale temporal and spatial variability in SO₂ and PM₁ peaks

The dense reference-grade network between 9 and 35 km from the eruption site (clusters G2 and G3) revealed fine-scale variability at these relatively distal sites. Five out of 6 stations on Reykjanes peninsula (SO₂ only) were north and northwest from the eruption site, within the most common wind direction (wind rose in Fig. B11). Despite only 3–16 km distance between these stations, two of them (G2-E and G2-F) recorded 25 and 31 SO₂ hourly mean exceedance events, respectively, while G2-B, G2-C and G2-D recorded between 0 and 6 events (Fig. 3). The dense regulatory monitoring network located 9–35 km from the eruption site (clusters G2 and G3) revealed fine-scale variability in SO₂ concentrations at these relatively distal locations. Five out of six stations on the Reykjanes peninsula (monitoring SO₂ only) were positioned north and northwest of the eruption site, within the most common wind direction (Figure A12). Despite being only 3–16 km apart, two of these stations—G2-E and G2-F—recorded 25 and 31 hourly SO₂ exceedance events, respectively, while G2-B, G2-C, and G2-D recorded between 0 and 6 events (Fig. 3). To test that this was not an artifact of some of the stations having been set up later than others during the eruption, we also counted the number of exceedance events from 7 May 2021, the date by which all G2 stations had become operational. The result was largely unchanged: the number of exceedance events remained higher at G2-E and F (7 and 26 events, respectively) and lower at G2-B, C, and D (0–6 events). To ensure this pattern was not an artifact of staggered station deployment, we recalculated exceedance events starting from 7 May 2021, the date by which all G2 stations were operational. The results remained consistent: G2-E and G2-F recorded 7 and 26 events, respectively, while G2-B, G2-C, and G2-D recorded between 0 and 6 events. The spatio-temporal difference between the ‘high-exceedance stations’ G2-E and G2-F, which were within 5 km distance of each other is also noteworthy: during the first 7 weeks of the eruption (19 March–7 May 2021) G2-E recorded 18 of its total 25 exceedance events, while G2-F recorded only 5 out of 31. The spatio-temporal difference between the two ‘high-exceedance’ stations—G2-E and G2-F, located within 5 km of each other—is also noteworthy. During the first seven weeks of the eruption (19 March–7 May 2021), G2-E recorded 18 of its 25 total exceedance events, while G2-F recorded only 5 of its 31. This likely reflects the control of the wind direction rather than topography as both stations were close to sea level, and demonstrates that the edges of the volcanic pollution cloud were sharply defined. Figure 7 illustrates one such episode of fine-scale variability in SO₂ concentrations between G2 stations (28–30 May 2021). During this event, the volcanic pollution cloud ‘migrated’ between the closely spaced stations G2-C, G2-D, and G2-E (separated by ~2 km). The plume first reached G2-C, then shifted to G2-D and G2-E, with G2-D recording nearly twice the peak concentration of G2-E. This demonstrates that the edges of the volcanic pollution cloud at ground level were sharply defined. (Pfeffer et al., 2024) The movement and sharp boundaries of the plume during the 28–30 May episode are shown in an animation in Supplementary Figure S1, based on a dispersion model used operationally for volcanic air quality advisories during the eruption by the IMO (Barsotti, 2020; Pfeffer et al., 2024). The model results are used here for qualitative purposes—as a binary yes/no indicator of potential plume presence at ground level. This is because the model has been shown to have a reasonable skill in predicting the general plume direction but relatively low accuracy in simulating ground-level SO₂ concentrations for the 2021 eruption (Pfeffer et al., 2024).

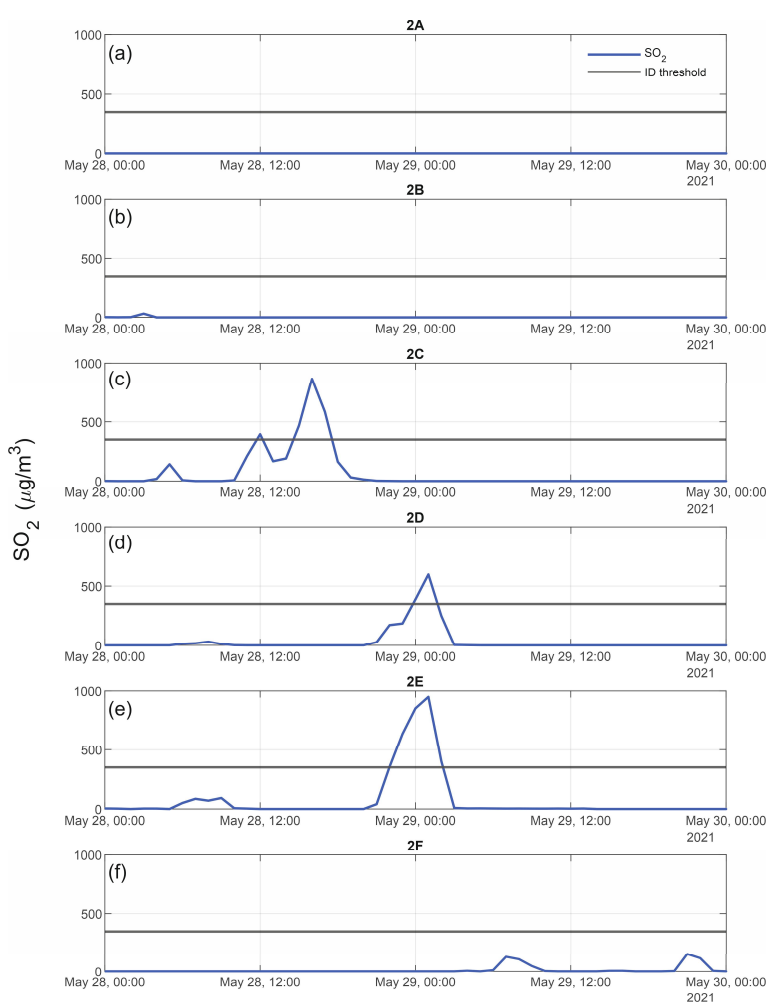


Figure 7: Spatial and temporal variability in SO_2 concentrations ($\mu\text{g}/\text{m}^3$, hourly-mean) between monitoring stations on the Reykjanes peninsula (G2) during 28–30 May 2021. The Icelandic Directive (ID) air quality threshold for hourly SO_2 concentrations ($350 \mu\text{g}/\text{m}^3$)

Formatted: Caption

735 is indicated by a black horizontal line. Panel (a): Station G2-A. Panel (b): Station G2-B. Panel (c): Station G2-C. Panel (d): Station G2-D. Panel (e): Station G2-E. Panel (f): Station G2-F. The map of the stations' locations is on Fig. 1.

Formatted: Font: (Default) Times New Roman

740 Reykjavík capital area stations (G3) were located 25–35 km from the eruption site and within <1 and 10 km from one another (Fig. 1). The most significant volcanic plume advection episode happened on 18–19 July 2021, when the G3 stations cumulatively recorded 21 SO₂ hourly mean air quality exceedance events out of the 23 recorded during the whole eruption.

745 This advection episode revealed how the concentrations of volcanic pollutants varied on a fine spatio-temporal scale. Stations in the Reykjavík capital area (G3), located 25–35 km from the eruption site and within <1–10 km of one another (Fig. 1), recorded fine-scale variability in pollutant concentrations—even at this relatively large distance from the source. The most significant volcanic plume advection episode occurred on 18–19 July 2021, during which the G3 stations cumulatively recorded 21 SO₂ hourly mean air quality exceedance events—out of the 23 total exceedances recorded throughout the entire

750 eruption. This episode revealed pronounced spatio-temporal variability in volcanic pollutant concentrations. Figures 7a–7d show the spatio-temporal resolution and ratios of SO₂ and PM as hourly means during this episode. We focus this discussion on PM₁ rather than PM_{2.5} and PM₁₀ because PM₁ more clearly represented the volcanic source compared to the other size fractions, as discussed in 3.1 and shown on Figs. 7e–7d. Both SO₂ and PM₁ were highly elevated above background concentrations during the advection episode at all G3 stations (Figs. 7a–7d). Figure 8 illustrates the variation in SO₂ and PM₁

755 abundances during this episode, shown as time series (Figs. 8a–8b) and as concentration ratios (Figs. 8c–8d). This discussion focuses on PM₁ rather than PM_{2.5} and PM₁₀ because PM₁ was more pronounced in the volcanic air pollution, as discussed in Section 3.1 and shown in Figs. 8c–8d. Both SO₂ and PM₁ were significantly elevated above background levels at all G3 stations

760 during the advection episode. Stations G3-A and G3-E were located <1 km of each other; during the 18–19 July episode G3-E recorded ~2 times higher maximum SO₂ concentrations than G3-A (480 and 250 µg/m³, respectively), and five SO₂ air quality threshold exceedance events while G3-A recorded zero (Figs. 2 and 7a). The fine scale spatio-temporal differences

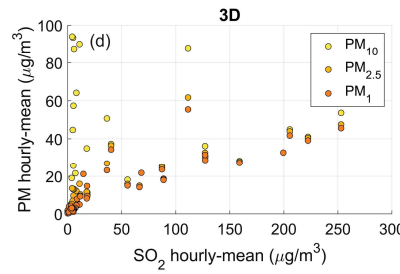
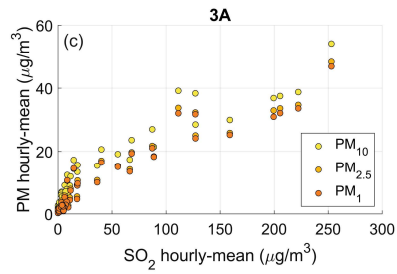
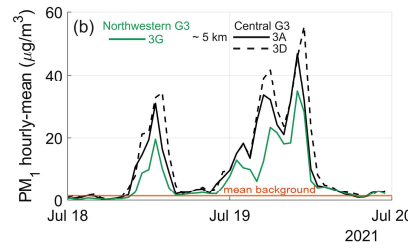
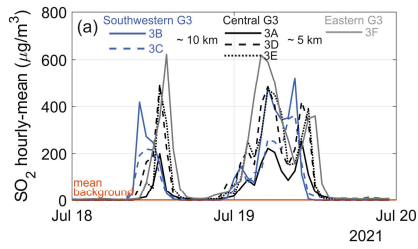
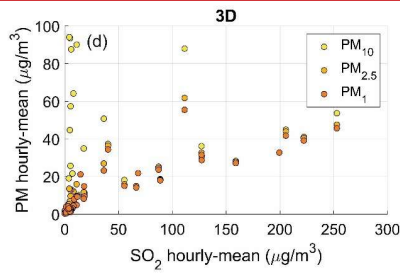
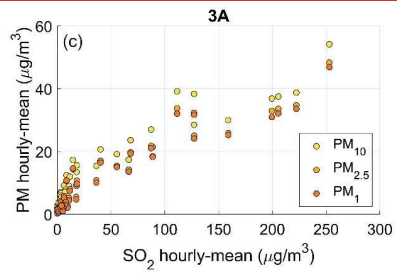
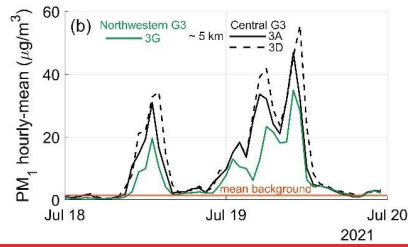
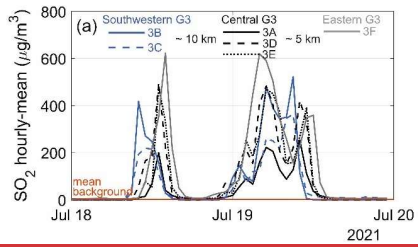
765 were also observed in PM₁; for example, G3-D recorded up to twice as high PM₁ hourly means than G3-G during the same advection episode (Fig. 7b). Stations G3-A and G3-E, located within 1 km of each other, showed notable differences: G3-E recorded a maximum SO₂ concentration of 480 µg/m³ and five exceedance events, while G3-A recorded a peak of 250 µg/m³ and no exceedances (Figs. 3 and 8a). Similar fine-scale differences were observed in PM₁; for example, G3-D recorded up to

770 twice the PM₁ hourly mean concentrations of G3-G during the same episode (Fig. 8b). The topographic elevation difference between G3 stations is unlikely to explain the spatial fluctuations as it is relatively small. Most of the G3 stations are located between 10 and 40 m above sea level (a.s.l.) and G3-F is at 85 m a.s.l.. One potential contributing factor could be channelling and/or downwash of air currents by urban buildings, a process that might be important for central Reykjavík locations, and requires further investigation, e.g. by fine-scale dispersion modelling, but is beyond the scope of this study. Topographic elevation differences are unlikely to explain this spatial variability, as most G3 stations are located between 10 and 40 m above sea level (a.s.l.), with G3-F at 85 m a.s.l. One potential contributing factor could be the channelling or downwash of air currents by urban buildings—a process that may be particularly relevant in central Reykjavík. This warrants further investigation, such

as through fine-scale dispersion modelling, but is beyond the scope of this study. (Pfeffer et al., 2024)(Pfeffer et al., 2024)(Barsotti, 2020; Pfeffer et al., 2024; Sokhi et al., 2022)Supplementary Figure S2 shows an animation of the simulated dispersion of volcanic SO₂ at ground level during the 18–19 July episode as simulated by the IMO model (Pfeffer et al., 2024). As discussed by Pfeffer et al. (2024), the dispersion model did not accurately simulate all ground-level pollution events, including this one—the largest SO₂ pollution episode in Reykjavík during the eruption. This highlights the challenges of accurately simulating ground-level dispersion of volcanic emissions from eruptions like Fagradalsfjall 2021, as well as other small but highly dynamic natural and anthropogenic sources (Barsotti, 2020; Pfeffer et al., 2024; Sokhi et al., 2022). High-resolution observational datasets, including those presented here, can support improvements in dispersion model performance.

Formatted: Font: (Default) +Headings (Times New Roman)

The relative proportions of SO₂ and PM₁ during the 18–19 July advection episode varied strongly between the two stations that measured both pollutants (G3-A and G3-D). The peak hourly mean SO₂ concentration differed by nearly a factor of two between the stations (Fig. 8a), whereas peak PM₁ hourly means differed by no more than 20% (Fig. 8b). The relative proportions of the two pollutants, SO₂ and PM₁, in the 18–19 July advection episode varied strongly between the two stations that measured both of them (G3-A and G3-D). The SO₂ peak hourly mean differed by nearly a factor of 2 between the two stations (Fig. 7a), but PM₁ peak hourly means only by a maximum of 20% (Fig. 7b). During the advection episode, both pollutants showed 3 principal concentration peaks. The first of the three principal concentration peaks (July 18 13:00) recorded the highest SO₂ concentration at station G3-D, and the last of the 3 pollution peaks (July 19 23:00) recorded the highest PM₁ concentration at the same station (Figs. 7a–7b). During the advection episode, both pollutants exhibited three principal concentration peaks. The first peak, on 18 July at 13:00, corresponded to the highest SO₂ concentration recorded at station G3-D. The final peak, on 19 July at 23:00, marked the highest PM₁ concentration at the same station (Figs. 8a–8b).



795 **Figure 87:** SO₂ and PM concentrations ($\mu\text{g}/\text{m}^3$, hourly-mean) during a ‘fresh’ volcanic plume advection episode in the Reykjavík capital area (G3) on 18–19 July 2021. Stations G3-A to G3-F are regulatory monitoring sites, and the figure indicates their respective locations within Reykjavík (southwestern, central, eastern, and northwestern), along with approximate distances between them. 3A to 3F are names of reference-grade stations and the figure indicates their respective locations within Reykjavík (southwestern, central, eastern, and northwestern) and the approximate distance between them. Panel (a): SO₂ hourly-means timeseries. Panel (b): PM₁ hourly-means timeseries. Panel (c): Scatter plot between of concentrations of SO₂ and PM₁₀, PM_{2.5} and PM₁ at station 3A, which measured all of these four pollutants. Panel (d): Scatter plot between of concentrations of SO₂ and PM₁₀, PM_{2.5} and PM₁ at station 3D, which measured all of these four pollutants.

Formatted: Superscript

800 We also examined the fluctuations in SO₂ and PM₁ during an advection episode of a chemically mature plume locally known as ‘móða’, or ‘vog’ in English (volcanic smog) in Reykjavík capital area July 1–7 2021 (Fig. 8a–8d). A chemically mature plume has undergone significant gas to particle conversion of sulphur in the atmosphere and, as shown by Ilyinskaya et al. 2017, may be advected into the populated area some days after the initial emission. We also examined fluctuations in SO₂ and PM₁ during an advection episode of a chemically mature volcanic plume—locally known as *móða* (or *vog* in English, meaning 805 volcanic smog)—in the Reykjavík capital area between 1 and 7 July 2021 (Figs. 9a–9d). A chemically mature plume has undergone significant gas-to-particle conversion of sulfur in the atmosphere and, as shown by Ilyinskaya et al. (2017), may be advected into populated areas several days after the initial emission. The mature plume (Figs. 8e–8d) has a higher PM/SO₂ ratio than a fresh plume (Figs. 7e–7d), and SO₂ is elevated to above background levels to a variable degree, sometimes only slightly (Ilyinskaya et al., 2017). Conditions which would typically facilitate the generation of móða and its accumulation are 810 low wind speed, high humidity and intense solar radiation. Based on these factors, the 1–7 July episode was identified by IMO at the time of the event as móða, and a public air quality advisory was issued. Compared to a fresh plume (Figs. 8c–8d), the mature plume (Figs. 9c–9d) is characterized by a higher PM/SO₂ ratio, with SO₂ elevated above background levels to a variable degree—sometimes only slightly (Ilyinskaya et al., 2017). Conditions that typically facilitate the formation and accumulation 815 of móða include low wind speeds, high humidity, and intense solar radiation. Based on these factors, the 1–7 July episode was identified by the Icelandic Meteorological Office (IMO) as *móða* at the time of the event, and a public air quality advisory was issued. Figs. 8e–8d shows that during the móða event PM₁ is frequently elevated without a correspondingly high increase in SO₂. The highest peaks of SO₂ were well-defined but PM₁ was highly elevated above background levels throughout the whole 820 period with less prominent individual concentration peaks. It is possible that PM₁ grounds more persistently than SO₂, which could be tested in follow-on work by dispersion modelling with high vertical resolution near ground level. Figures 9c–9d show that during the móða episode, PM₁ was frequently elevated without a correspondingly high increase in SO₂. While SO₂ peaks were well-defined, PM₁ remained consistently elevated above background levels throughout the entire episode, with less prominent individual concentration peaks. This suggests that PM₁ may ground more persistently than SO₂—an observation that could be tested in future studies using high-resolution dispersion modelling near the surface.

Formatted: Caption

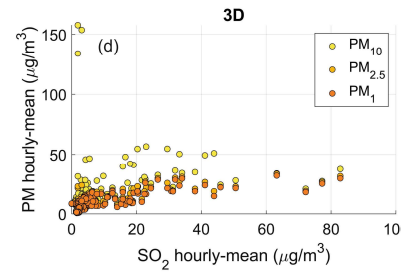
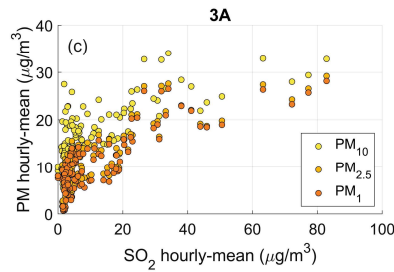
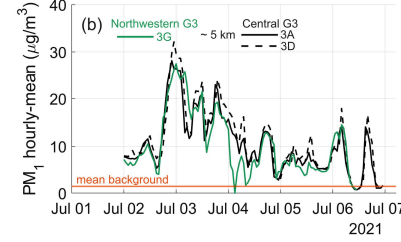
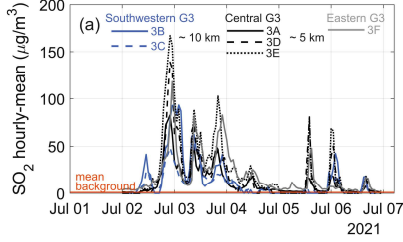
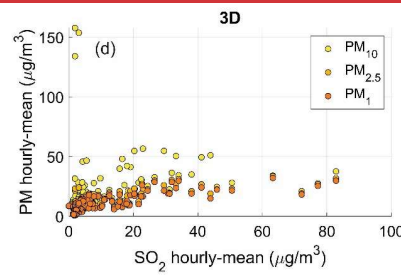
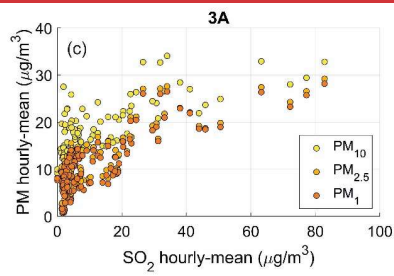
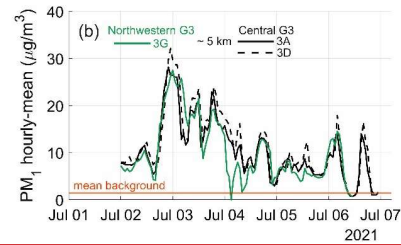
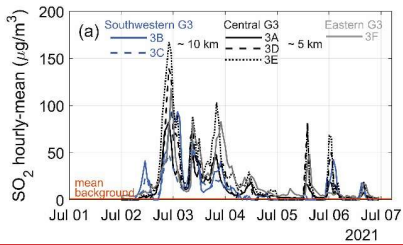


Figure 28: SO₂ and PM concentrations (µg/m³) during a ‘mature’ volcanic plume advection episode in Reykjavík capital area (G3) 1-7 July 2021. 3A to 3F are names of **reference-grade regulatory** stations and the figure indicates their respective locations within Reykjavík (southwestern, central, eastern, and northwestern) and the approximate distance between them. Panel (a): SO₂ hourly-means **timeseries** **time series**. Panel (b): PM₁ hourly-means **timeseries** **time series**. Panel (g): Scatter plot between concentrations of SO₂ and PM₁₀, PM_{2.5} and PM₁ at station 3A, which measured all of these pollutants. Panel (h): Scatter plot between concentrations of SO₂ and PM₁₀, PM_{2.5} and PM₁ at station 3D, which measured all of these pollutants.

3.5 **Estimates of potential population exposure to volcanic air pollution and implications for health impacts**

3.5.1 Exposure of residents

We considered the frequency of exposure in populated areas to SO₂ levels above air quality thresholds (350 µg/m³ hourly-mean) (Carlsen et al., 2021a, b). Evidence-based air quality thresholds for PM₁ do not yet exist, however, as shown in previous sections (e.g. Figs. 7 and 8), volcanic advection episodes contained SO₂, PM₁ and PM_{2.5} (and to a less significant extent, PM₁₀) and therefore people exposed to elevated levels of volcanic SO₂ were most likely also exposed to elevated levels of fine PM. We assessed the frequency of exposure to SO₂ concentrations above the ID air quality threshold (350 µg/m³ hourly-mean) in populated areas. Based on available evidence in volcanic areas, exceedances of this threshold are associated with adverse health effects (Carlsen et al., 2021a, b). Individuals exposed to elevated concentrations of volcanic SO₂ were also exposed to elevated levels of fine particulate matter, since the volcanic pollution episodes typically contained elevated levels of SO₂, PM₁ and PM_{2.5}—and to a lesser extent, PM₁₀ (Figs. 8 and 9). The exceedance of the SO₂ air quality threshold is therefore a proxy for exposure to elevated SO₂ and PM concentrations.

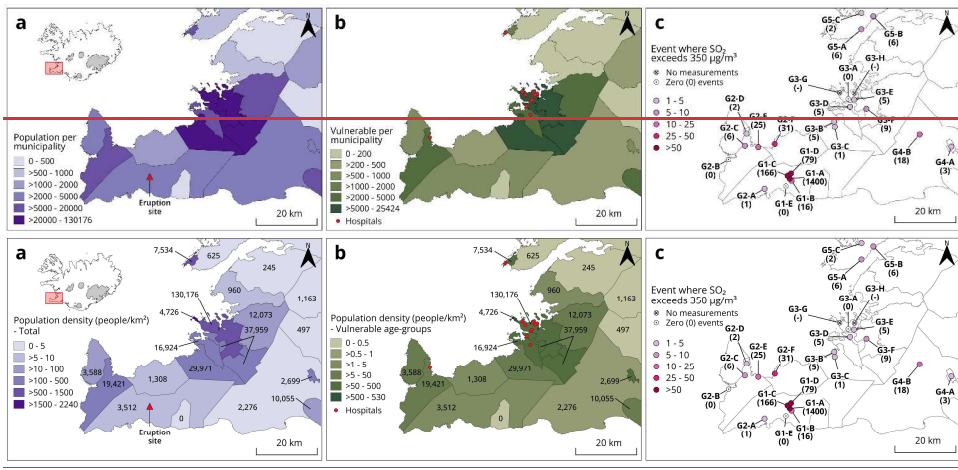
Formatted: Subscript

Formatted: Subscript

Data on the Icelandic population in the year 2020 were obtained from [Statistics Iceland \(2022\)](#) and were considered representative for 2021. Population data were obtained for each municipality of Iceland, both the total municipality population as well as population by age demographics. In 2020, Iceland had a population of 369,000. Of the total population, 6% and 15% of the population were in the age groups of ≤ 4 and ≥ 65 years, respectively, which have been shown to be more vulnerable to volcanic air pollution (Carlsen et al., 2021b, a). Population data for Iceland in the year 2020 were obtained from [Statistics Iceland \(2022\)](#) and were considered representative for 2021. Data were collected at the municipal level and included both total population and age-specific demographics. Municipality-level population datasets are relatively easy to obtain and are therefore frequently used in population exposure analyses (Caplin et al., 2019), but there are limitations to the resolution due to significant fine-scale spatial variations such as reported in this study.

In 2020, Iceland had a population of 369,000. Of this total, 6% were aged ≤ 4 years and 15% were aged ≥ 65 years—age groups which have been shown to be more vulnerable to volcanic air pollution (Carlsen et al., 2021b, a). There were 263,000 people, equating to 71% of the total population, within 50 km of the Fagradalsfjall eruption site where most of the SO₂ air quality threshold exceedances occurred. Fig. 9 shows municipality level population data for this area, number of vulnerable age group individuals, location of hospitals, and the number of ID air quality threshold exceedances at monitoring stations. A total of

860 [263,000 people—equivalent to 71% of the national population—resided within 50 km of the Fagradalsfjall eruption site, where most SO₂ air quality threshold exceedances occurred. Figure 10 presents municipality-level population data for this area, including total population and density, the number and density of individuals in vulnerable age groups, the locations of hospitals, and the number of ID air quality threshold exceedances recorded at monitoring stations.](#)



865 **Figure 109: Potential exposure of the general population in the densely populated southwestern part of Iceland, including the Reykjavík capital area (G3) of Iceland to above-threshold SO₂ concentrations (350 µg/m³ hourly-mean). Population data are from Statistics Iceland for 2020. Panel (a): Population map. The number of residents and the population density at the municipality level. The number of residents is shown for each municipality, and the colour scale represents the population density at the municipality level (n of people/km² in each municipality) of the densely populated southwestern part of Iceland, including the Reykjavík capital area (area G3). Population data in this figure for 2020 from Statistics Iceland. Panel (b): Potentially vulnerable age groups (<4 years and ≥ 65 years of age). The number of people in the vulnerable age groups is shown for each municipality, and the colour scale represents the population density (n of people/km² in each municipality). The map also shows the Map of potentially vulnerable sub-populations (<4 years and ≥ 65 years of age) in each municipality. Location of hospitals is shown. Panel (c): Number of events times when the SO₂ concentrations exceeded the ID air quality threshold of 350 µg/m³ hourly-mean during the eruption period as measured by the monitoring regulatory stations in (areas G1, G2 and G3). Source and copyright of basemap and cartographic elements: Icelandic Met Office & Icelandic Institute of Natural History.**

Formatted: Font: *Italic*

Formatted: Superscript

870 [The Reykjavík capital area](#) The capital area had approximately 210,000 residents (60% of the total population), a high density of individuals in the more potentially more vulnerable age groups, and a large number of hospitals (area G3 on Fig. 109). Air quality stations in this densely populated capital area recorded between 0 and 9 threshold exceedance events during the eruption period. Fine-scale spatial differences in ground-level pollutant concentrations (see Section 3.4) may have played a critical role in determining people's exposure. For example, one of the largest hospitals in the country was located approximately equidistant (~2 km) from stations G3-A and G3-E, which recorded 0 and 5 SO₂ exceedance events, respectively. As a result, it remains unknown how frequently individuals at the hospital were exposed to above-threshold SO₂ levels. The

885 fine-scale spatial differences in ground level pollutant concentrations (section 3.4) were potentially very important for the total exposure. For example, one of the largest hospitals in the country was located equidistantly (~2 km) from stations G3-A and G3-E that recorded, respectively, 0 and 5 SO₂ exceedance events, so it is not known how frequently people at the hospital were exposed to above threshold levels. Similarly, the hospital closest to the eruption site (20 km distance) was located in between two air quality monitoring stations (G2-D and G2-E) that recorded very different number of SO₂ exceedance events
890 ~2 and 25, respectively (Fig. 9). Similarly, the hospital closest to the eruption site—located about 20 km away—was situated between two monitoring stations, G2-D and G2-E, which recorded markedly different numbers of exceedance events: 2 and 25, respectively (Fig. 10). These examples highlight the importance of spatial resolution in air quality monitoring for accurately assessing population exposure.

895 With respect to nationwide public health impacts, it was fortunate that the volcanic pollutants were predominantly transported to the north and northwest of the eruption site, likely reducing the number of SO₂ pollution episodes in the densely populated capital to the northeast of the eruption site. (Pfeffer et al., 2024) The most frequent population exposure to potentially unhealthy levels of SO₂ occurred predominantly within a 20 km radius of the volcanic eruption site, in the municipalities on the Reykjanes peninsula, with up to 31 exceedance events (area G2 on Fig. 9). The most frequent exposure to potentially unhealthy SO₂ levels
900 occurred predominantly within a 20 km radius of the eruption site, particularly in municipalities on the Reykjanes Peninsula.

900 In this area (G2, Fig. 10), up to 31 exceedance events were recorded—surpassing the annual threshold of 24 exceedances (*p* = 24). Individuals who spent their working hours at some distance from their place of residence may have been exposed to different levels of volcanic pollution than can be estimated from exposure analysis based on residency. For example, station G2-A in the township of Grindavík recorded one exceedance event, but many of Grindavík's residents worked at Keflavík airport which experienced higher levels of SO₂ pollution (5 events at G2-C, Fig. 9). The reverse may have applied for those residents of Vogar (station G2-E, 25 events) who worked in the Reykjavík capital area where a lower number of exceedance events was observed (0–9 events). The estimated exposure of children was likely more accurate than for adults because most children go to schools within walking distance or minimal commuting distance from their homes. The same applies to long-term hospital inpatients. (Carlsen et al., 2021a) However, exposure estimates based solely on place of residence may not fully capture individual exposure, especially for working adults who commute. For example, station G2-A in the township of Grindavík recorded only one exceedance event, yet many residents worked at Keflavík Airport, where higher SO₂ levels were observed (five exceedance events at station G2-C, Fig. 10). Conversely, residents in the town of Vogar (station G2-E, 25 exceedance events) who commuted to the Reykjavík capital area—where fewer exceedances were recorded (0–9 events)—may have experienced lower actual exposure than estimated based on residence alone. In contrast, exposure estimates for
910 children are likely more accurate, as most attend schools within walking distance or a short commute from home. The same applies to long-term hospital inpatients, whose exposure is closely tied to the location of the healthcare facility.

Formatted: Font: Italic

From a nationwide public health perspective, it was fortunate that volcanic pollutants were predominantly transported to the north and northwest of the eruption site. This atmospheric transport pattern likely mitigated the frequency of SO₂ pollution episodes in the densely populated capital area, situated to the northeast of the eruption site. Supplementary Figure S3 illustrates the total probability of above-threshold SO₂ concentrations at ground level during the eruption, as simulated by the IMO dispersion model (Pfeffer et al., 2024). As outlined in Section 3.4, these simulations are used here solely to provide a qualitative indication of the broad plume direction at ground level. The modelled dispersion patterns are consistent with observational data, indicating that the plume most frequently grounded to the north and northwest of the eruption site, and more rarely in the capital area (Fig. S3).

Based on the available evidence, it is likely that the 2021 eruption may have resulted in adverse health impacts among exposed populations. Epidemiological studies by Carlsen et al. (2021a, b) on the 2014–2015 Holuhraun eruption demonstrated a measurable increase in healthcare utilisation for respiratory conditions in the Reykjavík capital area, associated with the presence of the volcanic plume. Exposure to above-threshold SO₂ concentrations was linked to approximately 20% increase in asthma medication dispensations and primary care visits. Furthermore, even modest increases in SO₂ levels were associated with small but statistically significant rises in healthcare usage—approximately a 1% increase per 10 µg/m³ SO₂—suggesting the absence of a safe lower threshold. During the Fagradalsfjall eruption, SO₂ concentrations in populated areas reached levels broadly comparable to those observed during the larger but more distal Holuhraun eruption. Consequently, similar health impacts may be expected, as inferred from the findings of Carlsen et al. (2021a, b). Holuhraun emissions led to 33 exceedances of the SO₂ air quality threshold in Reykjavík, with hourly-mean concentrations peaking at 1400 µg/m³ (Ilyinskaya et al., 2017). In comparison, the Fagradalsfjall eruption caused 31 exceedances, with a maximum of 2400 µg/m³ SO₂ recorded in the community of Vogar (station G2-F). Additionally, Fagradalsfjall caused SO₂ threshold exceedances across all monitored areas within approximately 50 km of the eruption site (areas G1–G5). (Ilyinskaya et al., 2017) (Carlsen et al., 2021b) By definition, there is no safe lower limit for the number of air quality exceedance events. Therefore, all areas that recorded above-threshold pollutant concentrations may have experienced adverse health effects. Furthermore, although the monitored regions in North and East Iceland (areas G6 and G7) did not register threshold exceedances, potential health impacts in these areas cannot be ruled out. As reported by Carlsen et al. (2021b), even relatively small, above-background increases in SO₂ concentrations during the Holuhraun eruption were associated with measurable health effects.

While each eruption has been relatively short-lived (duration from several days to several months), their cumulative effect on air pollution and health may potentially be chronic rather than acute and warrants investigation. (Carlsen et al., 2021a, b) Given the limited number and scope of health impact studies on previous volcanic eruptions, the potential health implications discussed here should be further investigated through dedicated epidemiological and/or clinical studies focused specifically on the Fagradalsfjall event. Moreover, existing health studies from volcanic regions have primarily concentrated on short-term exposure (hourly and daily), with a gap in research of potential long-term effects. Since the 2021 eruption, ten additional eruptions of similar style and in the same geographic area have occurred. Although each event has been relatively short-lived—

ranging from several days to several months—their cumulative impact on air quality and public health may be chronic rather than acute, and thus warrants comprehensive investigation.

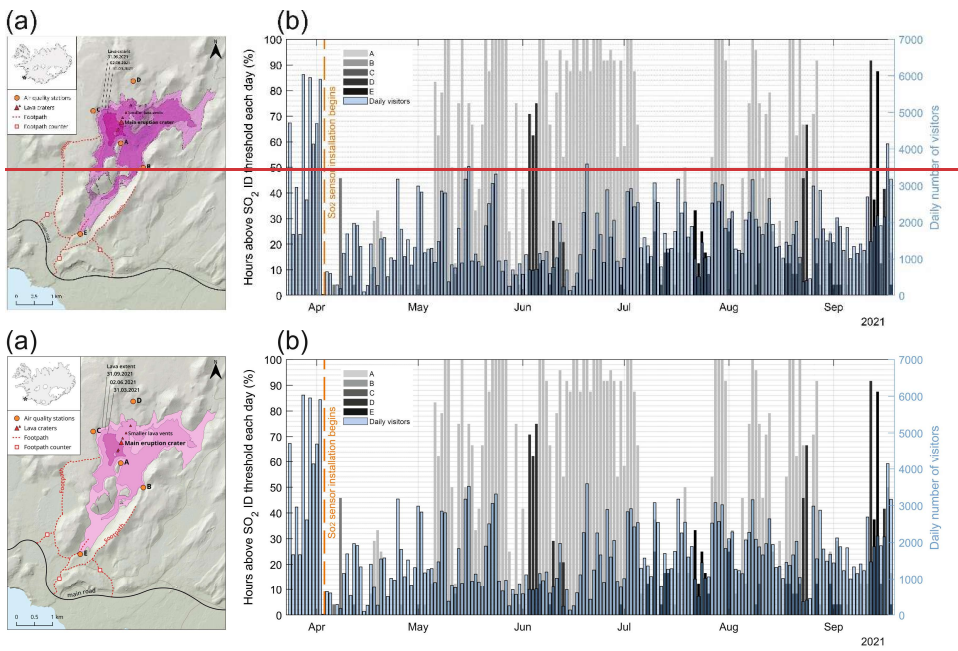
Carlsen et al. (2021a) found that when volcanic air pollution events from the Holuhraun eruption were successfully forecast and public advisories were issued, the associated negative health impacts were reduced compared to events that were not forecast. In Iceland, residential buildings are predominantly well-insulated concrete structures with double-glazed windows, offering substantial protection from outdoor air pollution. However, under normal conditions, windows are kept open for ventilation, facilitated by the availability of inexpensive geothermal heating. Additionally, it is common practice for infants to nap outdoors in prams, and for school-aged children to spend breaks outside. Public advisories included simple, easily implemented measures such as keeping windows closed and minimizing outdoor exposure for vulnerable individuals. Given that such basic societal actions have been shown to be effective, it is likely that further improvements in pollution detection—particularly enhancements in spatial resolution—and more effective communication strategies could provide additional protection to the population.

Municipality level population datasets are relatively easily available and therefore frequently used in population exposure analysis (Caplin et al., 2019). We show that for assessing air pollution exposure even from relatively distal sources, such as this volcanic eruption (20–55 km distance from source to impacted populated areas) there are challenges with using municipality level population data, as there are important fine-scale variations. Furthermore, even the exceptionally dense-reference grade air quality network in this part of Iceland was unable to fully spatially resolve the pollution dispersion and frequency of above threshold events.

3.5.2 Exposure of eruption site visitors

An interesting aspect of the eruption was that it was generally considered a very positive event by the Icelandic public (Ilyinskaya et al., 2024), and even though it took place in an uninhabited location the site became akin to a densely populated area due to the extremely high number of visitors. The mountainous area had no infrastructure before the eruption and was only accessible by rough mountain tracks. It was unsuitable for an installation of a regulatory air quality network but there were serious concerns about the hazard posed to the visitors by potentially very high SO₂ concentrations. A considerable effort was made by the national and local authorities to minimise the risk from volcanic and general outdoor hazards. A network of three footpaths was developed, starting at designated parking areas (Fig. 10a). The footpaths were modified several times over the course of the eruption as the lava field expanded and optimal viewing areas kept changing (Barsotti et al., 2023). In response, national and local authorities undertook significant efforts to mitigate hazards associated with both volcanic activity and general outdoor hazards. A network of three footpaths was established, originating from designated parking areas (Figure 11a). These footpaths were modified multiple times throughout the eruption as the lava field expanded and optimal viewing locations shifted (Barsotti et al., 2023). In this study, we evaluate the deployment of eruption-response LCS as a means to minimize exposure to hazardous SO₂ levels.

Formatted: Subscript



985

Figure 110: Visitor numbers and potential SO₂ exposure at the Fagradalsfjall eruption site (24 March – 18 September 2024). Eruption site visitor numbers 23 March – 19 September 2024 and potential exposure to above-threshold SO₂ concentrations estimated from eruption-site sensor dataLCS that were installed in April (stations A, B) and June (stations C, D, E). Panel (a): Topographic map of the Fagradalsfjall eruption site area showing the locations of the eruption craters, and the evolving extent of the lava field throughout the eruption. It also shows the locations of the five GI-SO₂-air-quality-sensorsLCS stations (A–E), the primary footpaths used by visitors which were the most likely locations for visitors, and the locations of the footpath visitor counters. Panel (b): Daily visitor counts and the number of hours per day during which SO₂ concentrations exceeded the ID air quality threshold (350 µg/m³ hourly-mean) at each station. SO₂ exceedance duration is expressed as a percentage of the day (number of hours/24 × 100) shows the number of visitors per day, and the number of hours where SO₂ was above ID air quality threshold (350 µg/m³ hourly-mean) at each station. The number of hours is shown as % of day duration (n of hours/24*100). Source and copyright of basemap and cartographic elements: Icelandic Met Office & Icelandic Institute of Natural History. Source and copyright of basemap and cartographic elements: Icelandic Met Office & Icelandic Institute of Natural History.

990

995

We estimated the number of people who visited the eruption site by using data from automated footpath counters installed by the Icelandic Tourist Board from 24 March 2021, one on each main footpath leading to the eruption site and viewpoints (Fig. 10a). The counters were PYRO-Box with an accuracy of 95% and a sensing capacity of 4 m in both directions (Eco Counter, 2021). Although the vast majority of visitors used the footpath network to reach the eruption site and viewpoints, some may have walked outside the bounds of the Eco Counter instrument range and so were not counted. There was also a number of people who landed at the eruption site on helicopter sightseeing tours who were not counted. Children who were carried, and

1005 people with permission to travel by vehicle (such as scientists and rescue teams) were also not included in the count. The visitor numbers presented here represent a minimum estimate. Automated footpath counters were installed by the Icelandic Tourist Board on 24 March 2021, with one device placed on each of the main footpaths leading to the eruption site and designated viewpoints (Fig. 11a). These counters (PYRO-Box, Eco Counter, 2021) have a reported accuracy of 95% and a sensing range of 4 meters. While the majority of visitors used the established footpath network, some individuals may have walked outside the detection range of the counters and were therefore not recorded. Additionally, visitors arriving via helicopter 1010 sightseeing tours, children being carried, and individuals with authorized vehicle access (e.g., scientists and rescue personnel) were not included in the count. The visitor numbers used here are therefore a minimum estimate. The data on visitors to the site did not include details of the age demographics and as such no identification of exposure of more-vulnerable age categories could be determined.

1015 During the footpath monitoring period (24 March to 18 September 2021), the site was visited by ~300,000 people, averaging 1,600 visitors per day. The visitor data also lacked demographic information, preventing any assessment of exposure among 1020 more vulnerable age groups. During the monitoring period (24 March to 18 September 2021), the eruption site was visited by approximately 300,000 people, averaging 1,600 visitors per day (Fig. 11b). The highest visitor numbers occurred in the early weeks of the eruption, coinciding with the Easter holiday period, with a daily average of 3,300 visitors and a peak of 6,000 on 1025 28 March.

1030 1020 The eruption-response SO₂ air quality sensors (G1) were set up along the same footpaths and we used these measurements to assess the potential exposure levels of the visitors (Fig. 10). This is based on the assumption that the concentrations measured at the stations are representative of the rest of the footpaths and other locations of the eruption site visited by people, and therefore includes considerable error margins. The highest visitor numbers were in the first weeks of the eruption that coincided with Easter vacation period, with a daily average of 3,300 visitors, and a peak of 6,000 visitors on March 28. G1 stations were not set up until 3 April, therefore we have no indication of the potential exposure during the most frequently visited period. Figure 10b shows the frequency of ID exceedance events (350 $\mu\text{g}/\text{m}^3$ hourly-mean SO₂) at each of the 5 monitoring stations, and the number of daily visitors counted on the footpaths. The likelihood of exposure to above-threshold SO₂ was predominantly in the vicinity of station G1-A, which recorded a cumulative total of 1600 hours above the threshold. Station G1-C had the second highest exposure with cumulative total 110 hourly-exceedances. The other three stations recorded relatively low number of exceedances, between 0 and 20 events. G1-C and G1-D were more frequently downwind of the active vents compared to the other G1 stations (wind rose in Fig. B11), and the local-scale topography played a role. In addition, based on our visual observations of this eruption, and comparable fissure eruptions, a plume from a fissure eruption can occasionally collapse and spread laterally. This leads to extremely high concentrations of SO₂ even at locations upwind of the volcanic vent. The five eruption-response LCS were strategically deployed along the main footpaths (Fig. 11a) to ensure proximity to visitors. Figure 11b shows the frequency of ID threshold exceedance events (350 $\mu\text{g}/\text{m}^3$ hourly-mean SO₂) recorded at each of the stations. Station G1-A registered the highest cumulative exposure, with a total of 1,600 hours above 1035 the threshold. Stations G1-B, G1-C, and G1-D recorded between 110 and 10 hours of exceedance, while G1-E did not register

any exceedances. Stations G1-C and G1-D were more frequently located downwind of the active vents, as supported by the wind rose diagram in Figure B11. Additionally, based on visual observations during this eruption and similar fissure eruptions, 1040 a volcanic plume can occasionally collapse and spread laterally. This leads to extremely high concentrations of SO₂ even at locations in close vicinity of but upwind of the volcanic vent.

Our estimate of visitors' exposure to above-threshold events is likely a worst-case scenario because of mitigation actions. The visitors were clearly advised to remain upwind of the active craters and the lava field, and the site was staffed by rescue team 1045 members and/or rangers carrying hand-held SO₂ monitors. When SO₂ concentrations exceeded threshold levels on the sensors, the visitors were urged to move into cleaner air. It is still quite likely that some visitors were exposed to unhealthy levels of SO₂ because the area was large enough that rangers with hand-held sensors were not near to all visitors and rapid changes in wind direction often brought SO₂ to areas that had clean air moments before. This is supported by anecdotal reports in the 1050 Icelandic media regarding individuals seeking health care after visiting the eruption site, reportedly feeling unwell from the gas emissions. Visitors were clearly advised to remain upwind of the active craters and lava field. The site was staffed by members of the rescue services and/or rangers, who carried handheld SO₂ LCS to supplement the semi-permanent sensor network. When SO₂ concentrations exceeded threshold levels, visitors were urged to relocate to areas with cleaner air. Although no formal health impact studies have been published to date, anecdotal reports in the Icelandic media suggest that 1055 only a small number of individuals sought medical attention after visiting the eruption site, citing symptoms related to gas exposure. This likely represents a very small proportion of the total visitor population. Instances of exposure to unhealthy SO₂ levels may have occurred for several reasons: not all visitors were in proximity to a sensor during their visit, and rapid shifts in wind direction or changes in eruption dynamics occasionally transported SO₂ into areas that had previously been unaffected. To obtain high-quality datasets with LCS, regular and frequent field calibration against regulatory instruments is essential. However, such calibration is typically feasible only during short-term campaigns at reasonably accessible locations. In this 1060 crisis-response scenario, the challenging terrain and limited accessibility of the eruption site precluded field calibration. The primary concerns associated with uncalibrated LCS in emergency contexts are false negatives—where the sensor underreports concentrations that exceed health thresholds—and false positives—where the sensor overreports concentrations that are actually below threshold. False negatives pose a problem by failing to alert individuals to hazardous conditions, while repeated false positives may undermine public trust and reduce compliance with safety advisories.

1065 Both issues can be mitigated by increasing the density of LCS coverage in each monitored area, as was done in this case by supplementing the semi-permanent network with handheld sensors. The likelihood of false positives is further reduced when the alert threshold is set relatively high, as is appropriate when the primary concern is short-term exposure to high concentrations. False negatives are less likely to result in non-compliance at sites used for short visits rather than permanent residence, as visitors are likely to be more willing and able to move.

1070 In conclusion, we suggest that the deployment of the LCS network contributed meaningfully to reducing the SO₂ hazard at the eruption site, given the high frequency of above-threshold SO₂ concentrations and the high number of people. Such networks

Formatted: Subscript

Formatted: Subscript

are recommended in comparable crisis-response scenarios, provided that careful consideration is given to how the data and resulting alerts are interpreted and communicated. However, their applicability may be less suitable in contexts where chronic exposure among permanent residents is the primary concern.

1075 The footpath network leading to the eruption viewpoints included an elevation ascent of 200 m, so visitors were undergoing physical exertion with elevated breathing and heart rate while they were within 3 km of the eruption. High levels of physical exertion during exposure to air pollution can increase the exposure of the respiratory system which may result in more significant health impacts (Koenig et al., 1983; Qin et al., 2019).

4 Conclusions

1080 The 2021 eruption of Fagradalsfjall marked the onset of a prolonged eruptive phase on the Reykjanes peninsula, with ten subsequent eruptions occurring through to the time of writing, and continued volcanic unrest. Our findings demonstrate that even a relatively small volcanic event, such as the 2021 eruption, can lead to significant air pollution of SO₂ and PM. The Fagradalsfjall 2021 eruption was the beginning of a prolonged eruptive period on the Reykjanes peninsula, which is ongoing at the time of writing. All investigations into the recent eruptions may prove useful for risk reduction efforts for years, and 1085 generations to come. Due to its proximity to densely populated areas, the Fagradalsfjall eruption caused elevated pollutant concentrations, and air quality threshold exceedances comparable to those observed during the much larger Holuhraun eruption of 2014–2015. These results suggest that the Fagradalsfjall eruption may have contributed to measurable adverse health effects, warranting further public health investigations. Moreover, the high frequency of eruptions in this region since 2021 raises the 1090 possibility of chronic, low-level air pollution, which should also be examined, particularly given that the ongoing ‘Reykjanes Fires’ eruptions may continue for several generations.

We showed that even Iceland’s exceptionally dense, reference-grade air quality monitoring network was insufficient to fully capture the fine-scale spatial variability of volcanic air pollution episodes. We recommend augmenting existing networks with well-calibrated low-cost sensors (LCS) to enhance spatial coverage, particularly in sensitive locations such as schools and hospitals, where vulnerable populations may be at greater risk. Previous studies on the Holuhraun eruption have demonstrated 1095 that public advisories on volcanic air pollution can serve as effective health protection measures. Therefore, improving the spatial resolution of air quality monitoring may further enhance public health outcomes by enabling more targeted and timely advice.

1100 Understanding the volcanic air pollution in a uniquely Icelandic event like the Reykjanes Fires has important implications for how we manage and prepare for other eruptions globally. The fine temporal and spatial variability in the volcanic pollution dispersion that we have discovered in this study calls for further investigation in eruptions in Iceland and other areas exposed to volcanic activity.

105 Understanding the volcanic air pollution in a uniquely Icelandic event like the Reykjanes Fires has important implications for how we manage and prepare for other eruptions globally. The fine-scale temporal and spatial variability in pollution dispersion identified in this study highlights the need for further investigation—not only in future Icelandic eruptions but also in other regions exposed to volcanic activity. Enhanced understanding of these dynamics can inform more effective monitoring strategies and public health responses worldwide.

110 We show that even the exceptionally dense reference grade air quality monitoring network in Iceland could not fully resolve the fine spatial fluctuations in volcanic air pollution episodes. We suggest that air quality networks are augmented, for example with well-calibrated lower-cost sensors, so that increased monitoring can be put in place to protect the most vulnerable individuals in the society, such as at schools and hospitals.

Table S1

1115 Excel file ‘Table_S1.xlsx. Information about instrumentation, data completeness, data exclusion, etc, for each SO₂ and PM monitoring station. Summary statistics for SO₂ (hourly-means), PM₁₀, PM_{2.5} and PM₁ (daily-means) data during the background and eruption periods. SO₂-concentration data (μg/m³) reported to 2 s.f. Excel file ‘Table_S1.xlsx. Information about instrumentation, data completeness, data exclusion, etc, for each SO₂ and PM monitoring station. Summary statistics for SO₂ (hourly-means), PM₁₀, PM_{2.5} and PM₁ (daily-means) data during the background and eruption periods. SO₂ concentration data (μg/m³) reported to 2 s.f. Full raw dataset openly available for download from Environment Agency of

1120 Iceland <https://loftgaedi.is/en>.

Formatted: Subscript

Formatted: Subscript

Formatted: Subscript

Formatted: Superscript

Figure S1

1125 Animated simulation of the volcanic SO₂ concentration at ground level for the period 28 – 30 May 2021. The colour scale represents the simulated concentrations at ground level (in μg/m³) but should be treated as only as a qualitative indication of plume presence at ground-level. The simulation was made by the CALPUFF dispersion model that was used operationally during the 2021 Fagradalsfjall eruption by the Icelandic Met Office. A detailed methodology of the dispersion simulations is in Pfeffer et al., (2024). The data presented in Figure S1 are unpublished data by the Icelandic Meteorological Office.

Figure S2

1130 Animated simulation of the volcanic SO₂ concentration at ground level for the period 18 – 20 July 2021. The colour scale represents the simulated concentrations at ground level (in μg/m³) but should be treated as only as a qualitative indication of plume presence at ground-level. The simulation was made by the CALPUFF dispersion model that was used operationally during the 2021 Fagradalsfjall eruption by the Icelandic Met Office. A detailed methodology of the dispersion simulations is in (Pfeffer et al., 2024). The data presented in Figure S2 are unpublished data by the Icelandic Meteorological Office.

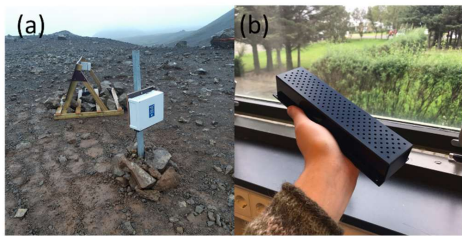
Figure S3

1135 Map of the total probability (%) of ground-level SO₂ concentrations exceeding the 350 μg/m³ air quality threshold during the 2021 Fagradalsfjall eruption. The map is based on dispersion simulations by the CALPUFF model that was used operationally by the Icelandic Meteorological Office. A detailed methodology of the dispersion simulations is in Pfeffer et al., (2024). The model results are used here for qualitative information about the plume direction (as a yes/no indication of the potential plume presence at ground level) because the model had a reasonable skill in predicting the broad plume direction but a relatively low

accuracy in simulating the concentrations of SO₂ at ground level (Pfeffer et al., 2024). The data presented in Figure S3 are unpublished data by the Icelandic Meteorological Office.

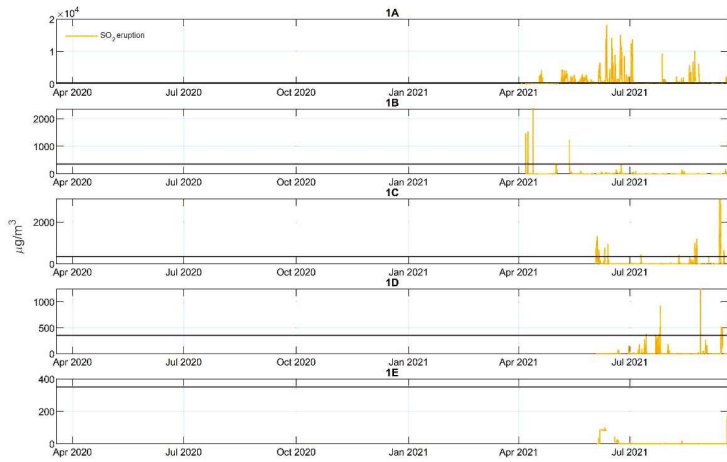
Appendix A**B**.

← **Formatted:** Left, Line spacing: single

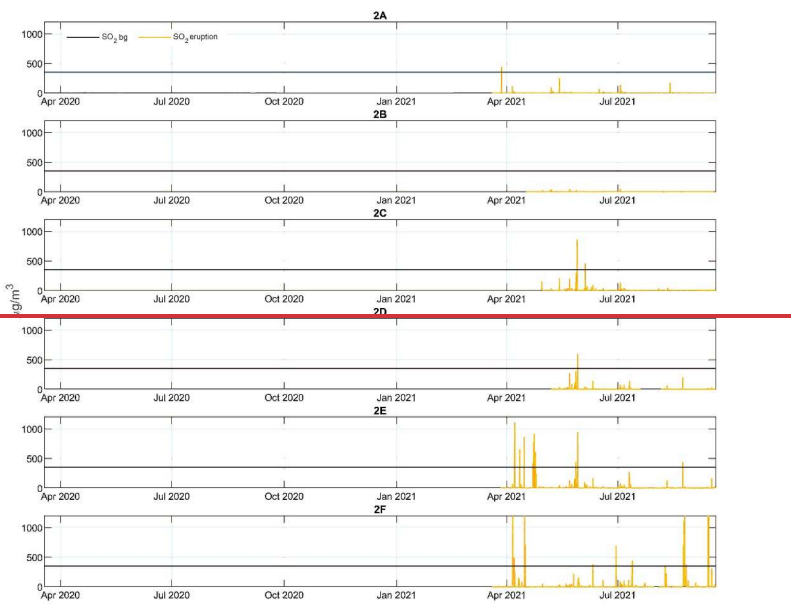


150 **Figure A1** Lower-cost sensors used for the Fagradalsfjall 2021 eruption. Panel (a) shows the instrument installed in the field. The station was powered by a solar panel (triangular trellis at the back of the photo). The air intake was underneath the instrument (the white box at the front of the image). Panel (b) shows the air intake of the sensor. The air intake was designed in-house at the IMO taking into account local conditions, in particular the weather and dust resuspension. The cover was custom-made from Plexiglass with the sensors are recessed behind it to be protected from dust, precipitation, and other potentially damaging environmental factors.

← Formatted: Normal



1160 Figure [ΔB21](#) Time series of hourly-mean concentrations SO_2 ($\mu\text{g}/\text{m}^3$), measured by the eruption site stations (G1 A-E) during the 2021 eruption. The stations were not in operation before the eruption and therefore there are no data on pre-eruptive background. The ID air quality threshold of $350 \mu\text{g}/\text{m}^3$ hourly-mean is shown on all panels with a black horizontal line. Note that the eruption-site sensors [LCS](#) have low accuracy and were only used in this study to indicate time periods that were over the ID threshold, the absolute concentration values were not included in the analysis.



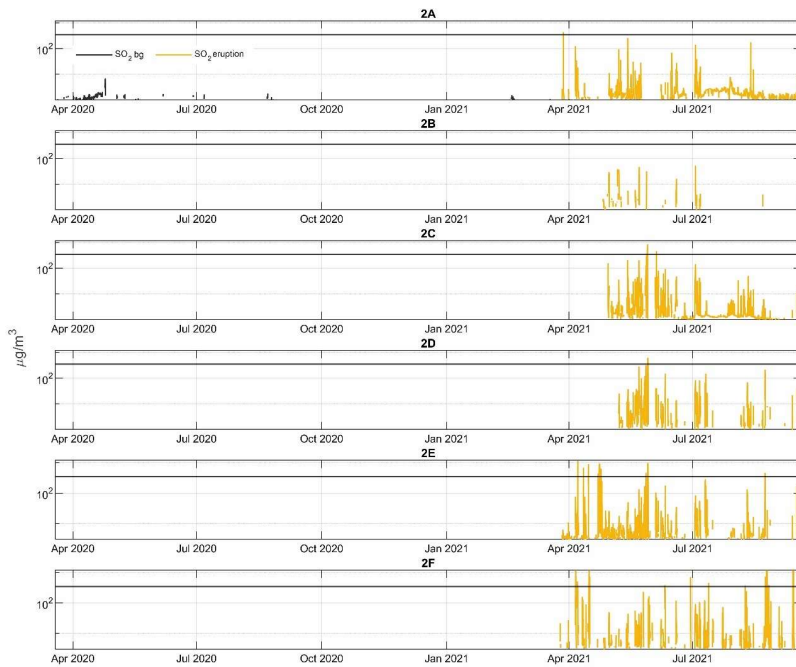
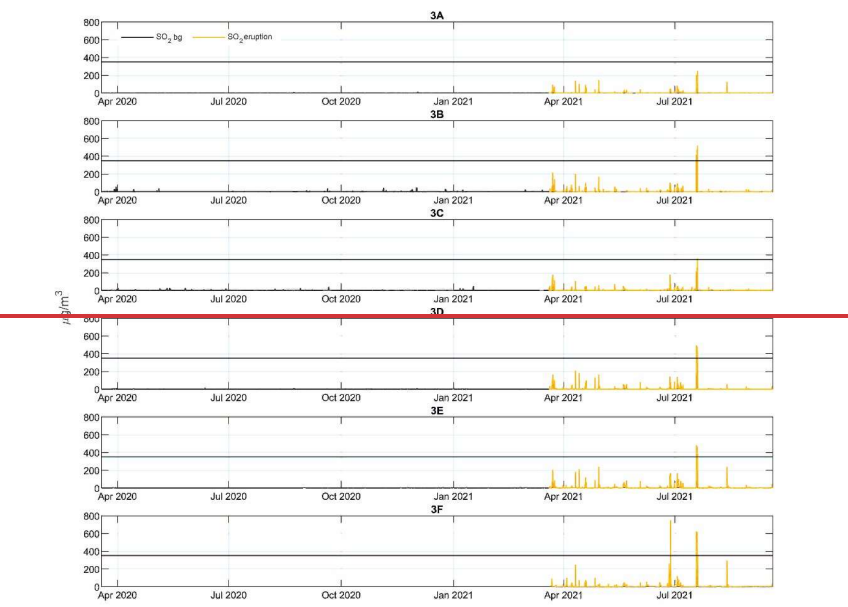


Figure AB32 Time-series of hourly-mean concentrations SO_2 ($\mu\text{g}/\text{m}^3$), measured by Reykjanes peninsula reference-grade regulatory air quality stations (G2 A-F) during the 2021 eruption and the non-eruptive background in 2020 (bg). The ID air quality threshold of $350 \mu\text{g}/\text{m}^3$ hourly-mean is shown on all panels with a black horizontal line. Please note the logarithmic y-axis scale.



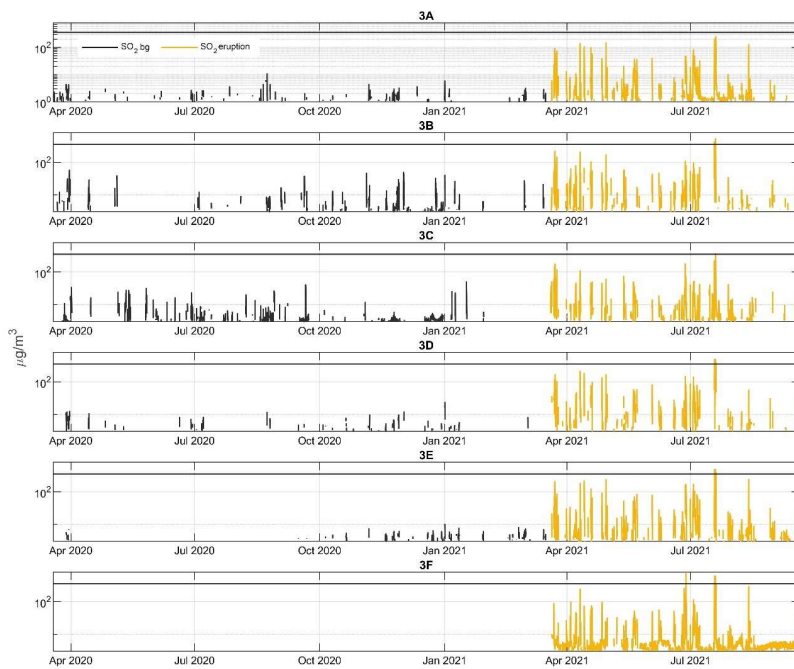
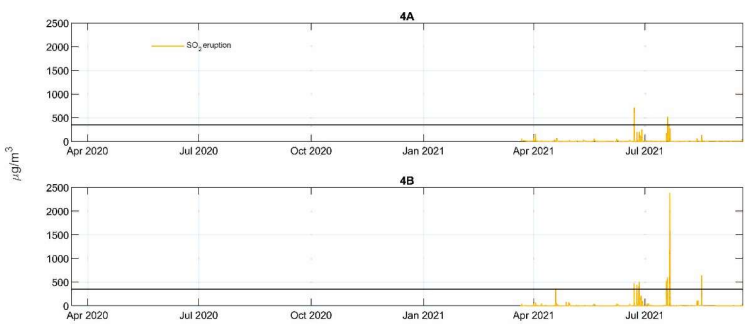


Figure [ΔB43](#) Time-series of hourly-mean concentrations SO_2 ($\mu\text{g}/\text{m}^3$), measured by Reykjavík capital area [reference-grade regulatory](#) air quality stations (G3 A-F) during the 2021 eruption and the non-eruptive background in 2020 (bg). The ID air quality threshold of $350 \mu\text{g}/\text{m}^3$ hourly-mean is shown on all panels with a black horizontal line. [Please note the logarithmic y-axis scale.](#)



180 **Figure AB54** Time-series of hourly-mean concentrations SO_2 ($\mu\text{g}/\text{m}^3$), measured in Southwest Iceland by **reference-grade** **regulatory** air quality stations (G4 A-B) during the 2021 eruption. The stations were not in operation before the eruption and therefore there are no data on pre-eruptive background. The ID air quality threshold of $350 \mu\text{g}/\text{m}^3$ hourly-mean is shown on all panels with a black horizontal line.

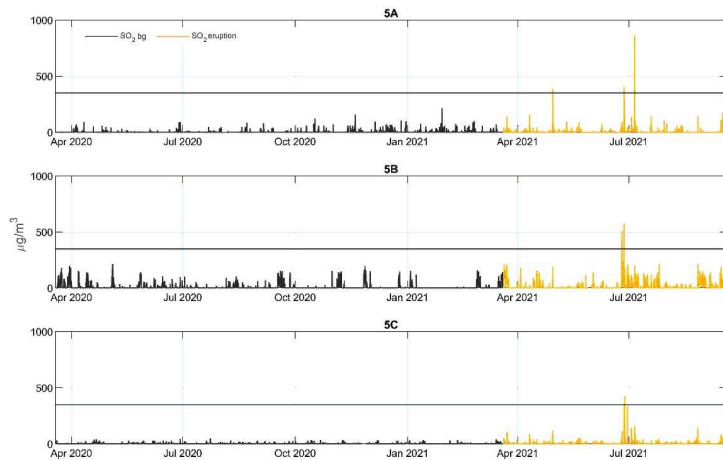
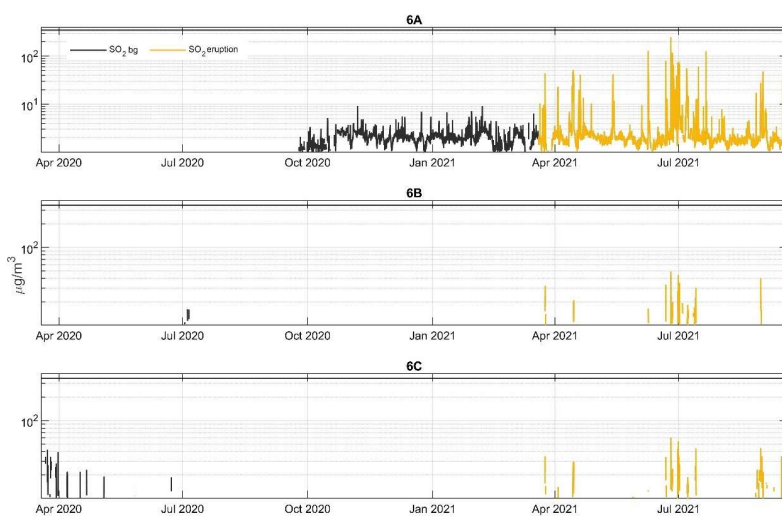
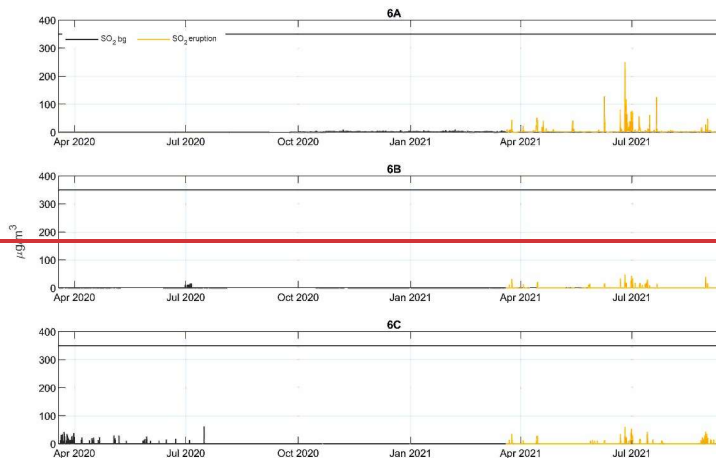


Figure [AB65 Time-series](#) of hourly-mean concentrations SO_2 ($\mu\text{g}/\text{m}^3$), measured in Hvalfjörður area by [reference-grade](#) [regulatory](#) air quality stations (G5 A-C) during the 2021 eruption and the non-eruptive background in 2020 (bg). The ID air quality threshold of $350 \mu\text{g}/\text{m}^3$ hourly-mean is shown on all panels with a black horizontal line.



1195 Figure [AB76 Time-series](#) of hourly-mean concentrations SO_2 ($\mu\text{g}/\text{m}^3$), measured in North Iceland by [reference-grade](#) [regulatory](#) air quality stations (G6 A-C) during the 2021 eruption and the non-eruptive background in 2020 (bg). The ID air quality threshold of $350 \mu\text{g}/\text{m}^3$ hourly-mean is shown on all panels with a black horizontal line. [Please note the logarithmic y-axis scale.](#)

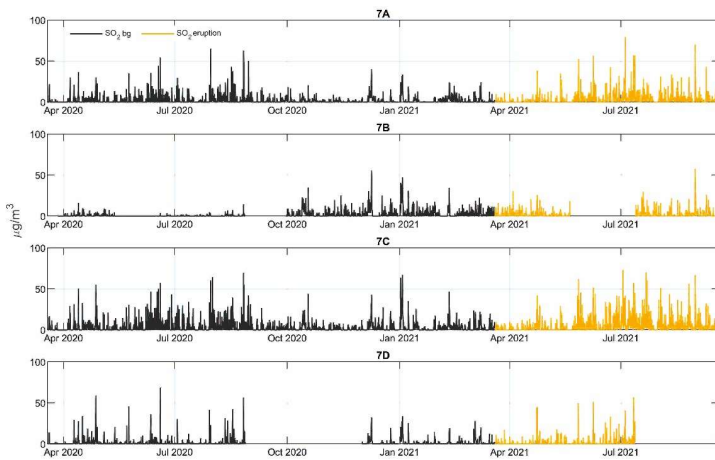


Figure AB87 Time-series of hourly-mean concentrations SO_2 ($\mu\text{g}/\text{m}^3$), measured in East Iceland by reference-grade regulatory air quality stations (G7 A-D) during the 2021 eruption and the non-eruptive background in 2020 (bg). The ID air quality threshold of $350 \mu\text{g}/\text{m}^3$ hourly-mean is shown on all panels with a black horizontal line.

1200

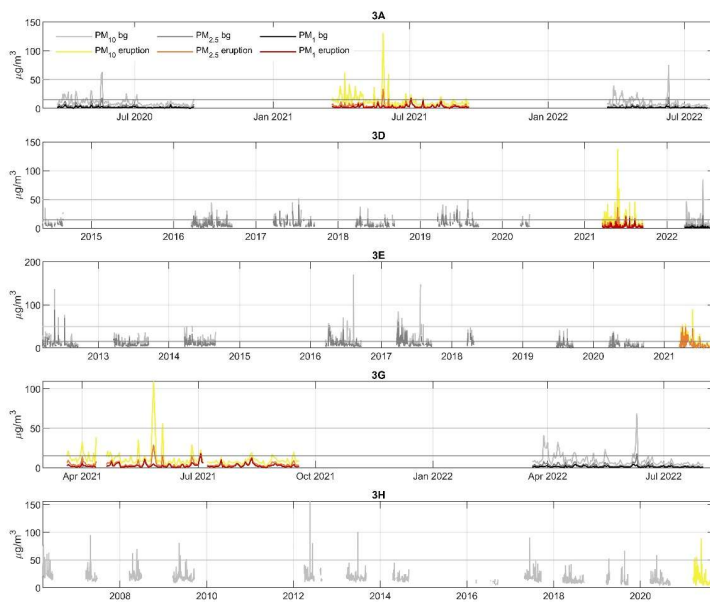


Figure AB28 Time-series of daily-mean concentrations of PM_{10} , $\text{PM}_{2.5}$ and PM_1 ($\mu\text{g}/\text{m}^3$) measured in Reykjavik capital area by reference-grade regulatory air quality stations (G3 A, D, E, G, H) during the 2021 eruption and in the non-eruptive background (bg). The amount of non-eruptive background data varies between stations based on their installation date. The figures only include data for the period 19 March 20:00 – 19 September 00:00 UTC in each year, i.e. the period corresponding to the calendar dates and months of the 2021 eruption. See main text for the justification of this approach. The figures show the ID air quality thresholds for PM_{10} and $\text{PM}_{2.5}$ of 50 and 15 $\mu\text{g}/\text{m}^3$ daily-mean, respectively as grey horizontal lines. For PM_1 , air quality thresholds have not been determined.

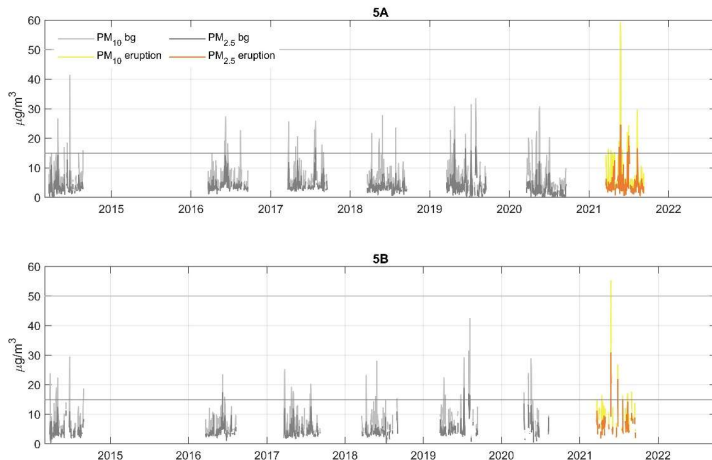
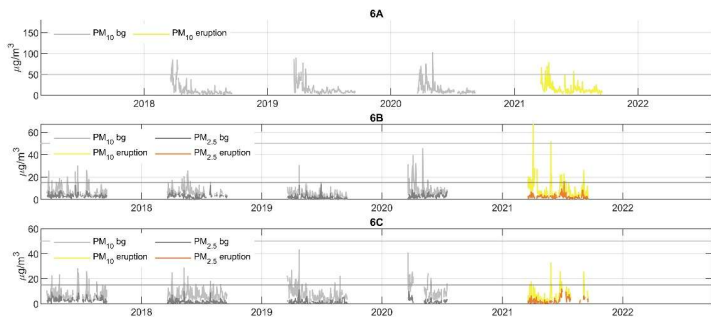


Figure [AB109](#) **Time-series** of daily-mean concentrations of PM_{10} , and $\text{PM}_{2.5}$ ($\mu\text{g}/\text{m}^3$) measured in Hvalfjörður area by **reference-grade** **regulatory** air quality stations (G5 A, B) during the 2021 eruption and in the non-eruptive background (bg). PM_1 was not measured at these stations. The amount of non-eruptive background data varies between stations based on their installation date. The figures only include data for the period 19 March 20:00 – 19 September 00:00 UTC in each year, i.e. the period corresponding to the calendar dates and months of the 2021 eruption. See main text for the justification of this approach. The figures show the ID air quality thresholds for PM_{10} and $\text{PM}_{2.5}$ of 50 and 15 $\mu\text{g}/\text{m}^3$ daily-mean, respectively as grey horizontal lines.

1215



1220 **Figure AB110** Time-series of daily-mean concentrations of PM_{10} , and $\text{PM}_{2.5}$ ($\mu\text{g}/\text{m}^3$) measured in North Iceland by
 1225 reference-grade regulatory air quality stations (G6 A, B, C) during the 2021 eruption and in the non-eruptive background (bg). PM_1
 was not measured at these stations. The figures only include data for the period 19 March 20:00 – 19 September 00:00 UTC in each
 year, i.e. the period corresponding to the calendar dates and months of the 2021 eruption. See main text for the justification of this
 approach. The figures show the ID air quality thresholds for PM_{10} and $\text{PM}_{2.5}$ of 50 and 15 $\mu\text{g}/\text{m}^3$ daily-mean, respectively as grey
 horizontal lines.

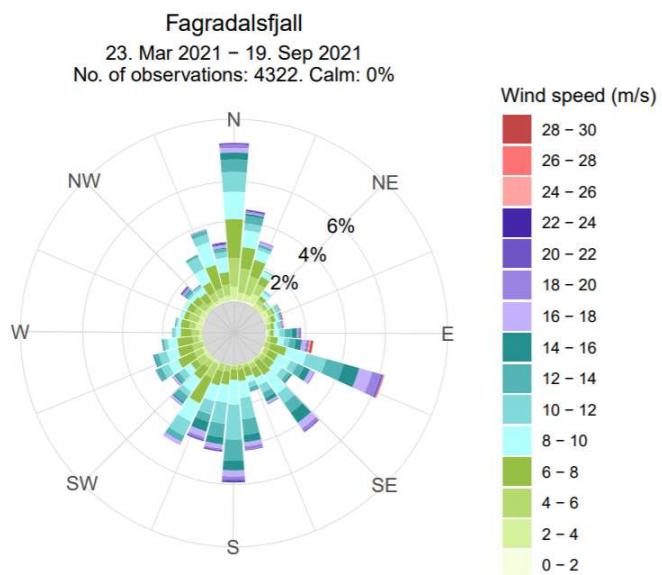


Figure A8.124 Wind rose shows wind direction (wind coming from) and wind speed measured by Icelandic Meteorological Office weather station at the Fagradalsfjall eruption site 23 March – 19 September 2021.

Data availability

Full dataset of measured SO₂, PM₁₀, PM_{2.5} and PM₁ concentrations is openly available for download from the Environment Agency of Iceland <https://loftgaedi.is/en>.

1235 Author contributions

RCWW performed the original data analysis and drafted the original manuscript and figures. SB, MAP, TR and AS contributed to data interpretation and manuscript drafting. EI finalised the data analysis, the manuscript and produced Figs. 2-7, 9 and Appendix AB1-B1-AB110. RHT produced Figs. 1, 8, and 9. TH, GMG and MAP designed, built and maintained IMO's measurement and data systems. TJ contributed access to and information on the reference graderegulatory AQ network and quality-controlled data. DF and RHT led on the ArcGIS ArcMap analysis methodology. GGS supplied the data from footpath counters. All coauthors contributed to draft review and editing.

Competing interests

The authors declare that they have no conflict of interest.

Acknowledgements

1245 The authors would like to thank Kristín Björg Ólafsdóttir from the Icelandic Meteorological Office for analysis of wind data and creation of the wind rose in Appendix AB Fig. AB124. Bogi Brynjar Björnsson at the Icelandic Meteorological Office is thanked for the preparation of Supplementary Figure S3. Microsoft Copilot (GPT-4) was used for English language editing, proofreading, and improving sentence clarity and structure; all content edited by Microsoft Copilot (GPT-4) was critically reviewed and approved by the authors.

1250 Financial support

RCWW was funded by the Leeds-York Natural Environment Research Council (NERC) Doctoral Training Partnership (DTP) NE/L002574/1, in CASE partnership with the Icelandic Meteorological Office. TJR was funded by the ANR Projet de Recherche Collaborative VOLC-HAL-CLIM (Volcanic Halogens: from Deep Earth to Atmospheric Impacts) ANR-18-CE01-0018, and Labex Orléans Labex VOLTAIRE (VOLatiles-Terre Atmosphère Interactions-Ressources et Environnement, 1255 ANR-10-LABX-100-0). EI acknowledges NERC Centre for Observation and Modelling of Earthquakes, Volcanoes and Tectonics (COMET+), a partnership between UK Universities and the British Geological Survey; NERC Highlight Topic V-PLUS NE/S00436X/1 and NERC Urgency Grant NE/Z000262/1 “Chemistry of emissions at lava-urban interfaces”.

References

1260 Apte, J. S. and Manchanda, C.: High-resolution urban air pollution mapping, *Science*, 385, 380–385, <https://doi.org/10.1126/science.adq3678>, 2024.

Barsotti, S.: Probabilistic hazard maps for operational use: the case of SO₂ air pollution during the Holuhraun eruption (Bárðarbunga, Iceland) in 2014–2015, *Bull. Volcanol.*, 82, 56, <https://doi.org/10.1007/s00445-020-01395-3>, 2020.

1265 Barsotti, S., Parks, M. M., Pfeffer, M. A., Óladóttir, B. A., Barnie, T., Titos, M. M., Jónsdóttir, K., Pedersen, G. B. M., Hjartardóttir, A. R., Stefansdóttir, G., Johannsson, T., Arason, Þ., Gudmundsson, M. T., Oddsson, B., Prastarson, R. H., Ofeigsson, B. G., Vogfjörd, K., Geirsson, H., Hjörvar, T., von Löwis, S., Petersen, G. N., and Sigurðsson, E. M.: The eruption in Fagradalsfjall (2021, Iceland): how the operational monitoring and the volcanic hazard assessment contributed to its safe access, *Nat. Hazards*, <https://doi.org/10.1007/s11069-022-05798-7>, 2023.

1270 Brauer, M., Roth, G. A., Aravkin, A. Y., Zheng, P., Abate, K. H., Abate, Y. H., Abbafati, C., Abbasgholizadeh, R., Abbasi, M. A., Abbasian, M., Abbasifard, M., Abbasi-Kangevari, M., ElHafeez, S. A., Abd-Elsalam, S., Abdi, P., Abdollahi, M., Abdoun, M., Abdulah, D. M., Abdulla, A., Abebe, M., Abedi, A., Abedi, A., Abegaz, T. M., Zuñiga, R. A. A., Abiodun, O., Abiso, T. L., Aboagye, R. G., Abolhassani, H., Abouzid, M., Aboye, G. B., Abreu, L. G., Abualruz, H., Abubakar, B., Abu-Gharbieh, E., Abukhadijeh, H. J. J., Aburuz, S., Abu-Zaid, A., Adane, M. M., Addo, I. Y., Addolorato, G., Adedoyin, R. A., Adekanmbi, V., Aden, B., Adetunji, J. B., Adeyeoluwa, T. E., Adha, R., Adibi, A., Adnani, Q. E. S., Adzigblie, L. A., Afolabi, A. A., Afolabi, R. F., Afshin, A., Afyouni, S., Afzal, M. S., Agampodi, S. B., Agbozo, F., Aghamiri, S., Agodi, A., Agrawal, A., Agyemang-Duah, W., Ahinkorah, B. O., Ahmad, A., Ahmad, D., Ahmad, F., Ahmad, N., Ahmad, S., Ahmad, T., Ahmed, A., Ahmed, A., Ahmed, A., Ahmed, L. A., Ahmed, M. B., Ahmed, S., Ahmed, S. A., Ajami, M., Akalu, G. T., Akara, E. M., Akbariabad, H., Akhlaghi, S., Akinosoglou, K., Akinyemiju, T., Akkaif, M. A., Akkala, S., Akombi-Inyang, B., Awaidy, S. A., Hasan, S. M. A., Alahdab, F., AL-Ahdal, T. M. A., Alalalmeh, S. O., Alalwan, T. A., Al-Aly, Z., Alam, K., Alam, N., Alanezi, F. M., Alanzi, T. M., Albakri, A., AlBataineh, M. T., Aldhaleei, W. A., et al.: Global burden and strength of evidence for 88 risk factors in 204 countries and 811 subnational locations, 1990–2021: a systematic analysis for the Global Burden of Disease Study 2021, *The Lancet*, 403, 2162–2203, [https://doi.org/10.1016/S0140-6736\(24\)00933-4](https://doi.org/10.1016/S0140-6736(24)00933-4), 2024.

1275 Butwin, M. K., von Löwis, S., Pfeffer, M. A., and Thorsteinsson, T.: The effects of volcanic eruptions on the frequency of particulate matter suspension events in Iceland, *J. Aerosol Sci.*, 128, 99–113, 2019.

1280 Caplin, A., Ghandehari, M., Lim, C., Glimcher, P., and Thurston, G.: Advancing environmental exposure assessment science to benefit society, *Nat. Commun.*, 10, 1236, <https://doi.org/10.1038/s41467-019-09155-4>, 2019.

Carlsen, H. K. and Thorsteinsson, T.: Associations between PM10 from Traffic, Resuspension, Sand Storms and Volcanic Sources and Asthma Drugs Dispensing, *In Review*, <https://doi.org/10.21203/rs.3.rs-1017409/v1>, 2021.

1285 Carlsen, H. K., Ilyinskaya, E., Baxter, P. J., Schmidt, A., Thorsteinsson, T., Pfeffer, M. A., Barsotti, S., Dominici, F., Finnbjörnsdóttir, R. G., Jóhannsson, T., Aspelund, T., Gislason, T., Valdimarsdóttir, U., Briem, H., and Gudnason, T.: Increased respiratory morbidity associated with exposure to a mature volcanic plume from a large Icelandic fissure eruption, *Nat. Commun.*, 12, 2161, <https://doi.org/10.1038/s41467-021-22432-5>, 2021a.

Carlsen, H. K., Valdimarsdóttir, U., Briem, H., Dominici, F., Finnbjörnsdóttir, R. G., Jóhannsson, T., Aspelund, T., Gislason, T., and Gudnason, T.: Severe volcanic SO_2 exposure and respiratory morbidity in the Icelandic population—a register study, *Environ. Health*, 20, 1–12, 2021b.

1290 Crawford, B., Hagan, D. H., Grossman, I., Cole, E., Holland, L., Heald, C. L., and Kroll, J. H.: Mapping pollution exposure and chemistry during an extreme air quality event (the 2018 Kilauea eruption) using a low-cost sensor network, *Proc. Natl. Acad. Sci.*, 118, 2021.

Crilley, L. R., Shaw, M., Pound, R., Kramer, L. J., Price, R., Young, S., Lewis, A. C., and Pope, F. D.: Evaluation of a low-cost optical particle counter (Alphasense OPC-N2) for ambient air monitoring, *Atmospheric Meas. Tech.*, 709–720, 2018.

1300 Felton, D., Grange, G., Damby, D., Bronstein, A., and Spyker, D.: Sulfur dioxide monitoring associated with the 2018 Kilauea Lower East Rift Zone Eruption, International Union of Toxicology (IUTOX) 15th International Congress of Toxicology, Honolulu, HI, USA, 2019.

Freire, S., Floreczyk, A. J., Pesaresi, M., and Sliuzas, R.: An Improved Global Analysis of Population Distribution in Proximity to Active Volcanoes, 1975–2015, *ISPRS Int. J. Geo-Inf.*, 8, 341, <https://doi.org/10.3390/ijgi8080341>, 2019.

1305 Gan, T., Chu, J., Bambrick, H., Guo, X., and Hu, W.: Long-term exposure to PM1 and liver cancer mortality: Insights into the role of smaller particulate fractions, *Ecotoxicol. Environ. Saf.*, 300, 118467, <https://doi.org/10.1016/j.ecoenv.2025.118467>, 2025.

1310 Gislason, S. R., Stefánsdóttir, G., Pfeffer, M. A., Barsotti, S., Jóhannsson, Th., Galeczka, I., Bali, E., Sigmarsson, O., Stefánsson, A., Keller, N. S., Sigurdsson, á., Bergsson, B., Galle, B., Jacobo, V. C., Arellano, S., Aiuppa, A., Jónasdóttir, E. B., Eiríksdóttir, E. S., Jakobsson, S., Guðfinnsson, G. H., Halldórrsson, S. A., Gunnarsson, H., Haddadi, B., Jónsdóttir, I., Thordarson, Th., Riishus, M., Högnadóttir, Th., Dürig, T., Pedersen, G. B. M., Höskuldsson, á., and Gudmundsson, M. T.: Environmental pressure from the 2014–15 eruption of Bárðarbunga volcano, Iceland, *Geochem. Perspect. Lett.*, 84–93, <https://doi.org/10.7185/geochemlet.1509>, 2015.

1315 Green, J. R., Fiddler, M. N., Holloway, J. S., Fibiger, D. L., McDuffie, E. E., Campuzano-Jost, P., Schroder, J. C., Jimenez, J. L., Weinheimer, A. J., Aquino, J., and others: Rates of wintertime atmospheric iceSO_2 oxidation based on aircraft observations during clear-sky conditions over the eastern United States, *J. Geophys. Res. Atmospheres*, 124, 6630–6649, 2019.

Guo, H., Li, X., Wei, J., Li, W., Wu, J., and Zhang, Y.: Smaller particular matter, larger risk of female lung cancer incidence? Evidence from 436 Chinese counties, *BMC Public Health*, 22, 344, <https://doi.org/10.1186/s12889-022-12622-1>, 2022.

1320 Horwell, C. J., Elias, T., Covey, J., Bhandari, R., and Truby, J.: Perceptions of volcanic air pollution and exposure reduction practices on the Island of Hawai'i: Working towards socially relevant risk communication, *Int. J. Disaster Risk Reduct.*, 95, 103853, <https://doi.org/10.1016/j.ijdrr.2023.103853>, 2023.

Icelandic Directive: Reglugerð um brennisteinsdioxíð, köfnunarefnisdioxíð og köfnunarefnisoxið, bensen, kolsýring, svifryk og blý í andrúmsloftinu, B-Deild, Nr.920, 2016.

1325 Ilyinskaya, E., Martin, R. S., and Oppenheimer, C.: Aerosol formation in basaltic lava fountaining: Eyjafjallajökull volcano, Iceland, *J Geophys Res.*, 117, D00U27, <https://doi.org/10.1029/2011JD016811>, 2012.

Ilyinskaya, E., Schmidt, A., Mather, T. A., Pope, F. D., Witham, C., Baxter, P., Jóhannsson, T., Pfeffer, M., Barsotti, S., Singh, A., Sanderson, P., Bergsson, B., McCormick Kilbride, B., Donovan, A., Peters, N., Oppenheimer, C., and Edmonds, M.: Understanding the environmental impacts of large fissure eruptions: Aerosol and gas emissions from the 2014–2015 Holuhraun eruption (Iceland), *Earth Planet. Sci. Lett.*, 472, 309–322, <https://doi.org/10.1016/j.epsl.2017.05.025>, 2017.

1330 Ilyinskaya, E., Mason, E., Wieser, P. E., Holland, L., Liu, E. J., Mather, T. A., Edmonds, M., Whitty, R. C. W., Elias, T., Nadeau, P. A., Schneider, D., McQuaid, J. B., Allen, S. E., Harvey, J., Oppenheimer, C., Kern, C., and Damby, D.: Rapid metal pollutant deposition from the volcanic plume of Kīlauea, Hawai'i, *Commun. Earth Environ.*, 2, 1–15, <https://doi.org/10.1038/s43247-021-00146-2>, 2021.

1335 Ilyinskaya, E., Snæbjarnarson, V., Carlsen, H. K., and Oddsson, B.: Brief communication: Small-scale geohazards cause significant and highly variable impacts on emotions, *Nat. Hazards Earth Syst. Sci.*, 24, 3115–3128, <https://doi.org/10.5194/nhess-24-3115-2024>, 2024.

Longo, B. M.: The Kilauea Volcano Adult Health Study, *Nurs. Res.*, 58, 2009.

Longo, B. M., Rossignol, A., and Green, J. B.: Cardiorespiratory health effects associated with sulphurous volcanic air pollution, *Public Health*, 122, 809–820, <https://doi.org/doi: DOI: 10.1016/j.puhe.2007.09.017>, 2008.

1340 Martin, R. S., Ilyinskaya, E., Sawyer, G. M., Tsanev, V. I., and Oppenheimer, C.: A re-assessment of aerosol size distributions from Masaya volcano (Nicaragua), *Atmos. Environ.*, 45, 547–560, <https://doi.org/doi: DOI: 10.1016/j.atmosenv.2010.10.049>, 2011.

Mason, E., Wieser, P. E., Liu, E. J., Edmonds, M., Ilyinskaya, E., Whitty, R. C. W., Mather, T. A., Elias, T., Nadeau, P. A., Wilkes, T. C., McGonigle, A. J. S., Pering, T. D., Mims, F. M., Kern, C., Schneider, D. J., and Oppenheimer, C.: Volatile metal emissions from volcanic degassing and lava–seawater interactions at Kilauea Volcano, Hawai‘i, *Commun. Earth Environ.*, 2, 1–16, <https://doi.org/10.1038/s43247-021-00145-3>, 2021.

1345 Mather, T. A., Pyle, D. M., and Oppenheimer, C.: Tropospheric volcanic aerosol, in: *Geophysical Monograph Series*, vol. 139, edited by: Robock, A. and Oppenheimer, C., American Geophysical Union, Washington, D. C., 189–212, <https://doi.org/10.1029/139GM12>, 2003.

1350 Pattantyus, A. K., Businger, S., and Howell, S. G.: Review of sulfur dioxide to sulfate aerosol chemistry at Kīlauea Volcano, Hawai‘i, *Atmos. Environ.*, 185, 262–271, <https://doi.org/10.1016/j.atmosenv.2018.04.055>, 2018.

Pfeffer, M. A., Arellano, S., Barsotti, S., Petersen, G. N., Barnie, T., Ilyinskaya, E., Hjörvar, T., Bali, E., Pedersen, G. B. M., Guðmundsson, G. B., Vogfjörð, K., Ranta, E. J., Óladóttir, B. A., Edwards, B. A., Mousallam, Y., Stefánsson, A., Scott, S. W., Smekens, J.-F., Varnam, M., and Titos, M.: SO₂ emission rates and incorporation into the air pollution dispersion forecast during the 2021 eruption of Fagradalsfjall, Iceland, *J. Volcanol. Geotherm. Res.*, 449, 108064, <https://doi.org/10.1016/j.jvolgeores.2024.108064>, 2024.

1355 Schmidt, A., Leadbetter, S., Theys, N., Carboni, E., Witham, C. S., Stevenson, J. A., Birch, C. E., Thordarson, T., Turnock, S., Barsotti, S., Delaney, L., Feng, W., Grainger, R. G., Hort, M. C., Höskuldsson, Á., Ialongo, I., Ilyinskaya, E., Jóhannsson, T., Kenny, P., Mather, T. A., Richards, N. A. D., and Shepherd, J.: Satellite detection, long-range transport and air quality impacts of volcanic sulfur dioxide from the 2014–15 flood lava eruption at Bárðarbunga (Iceland), *J. Geophys. Res. Atmospheres*, 2015JD023638, <https://doi.org/10.1002/2015JD023638>, 2015.

Sigurgeirsson, M. and Einarsson, S.: Reykjanes and Svartsengi volcanic systems, in: *Catalogue of Icelandic Volcanoes*, IMO, UI and CPD-NCIP, 2019.

1360 Sokhi, R. S., Moussiopoulos, N., Baklanov, A., Bartzis, J., Coll, I., Finardi, S., Friedrich, R., Geels, C., Grönholm, T., Halenka, T., Ketzel, M., Maragkidou, A., Matthias, V., Moldanova, J., Ntziachristos, L., Schäfer, K., Suppan, P., Tsegas, G., Carmichael, G., Franco, V., Hanna, S., Jalkanen, J.-P., Velders, G. J. M., and Kukkonen, J.: Advances in air quality research – current and emerging challenges, *Atmospheric Chem. Phys.*, 22, 4615–4703, <https://doi.org/10.5194/acp-22-4615-2022>, 2022.

Statistics Iceland: Average annual population by municipality, age and sex 1998–2022 - Current municipalities, 2022.

1365 Stewart, C., Damby, D. E., Horwell, C. J., Elias, T., Ilyinskaya, E., Tomašek, I., Longo, B. M., Schmidt, A., Carlsen, H. K., Mason, E., Baxter, P. J., Cronin, S., and Witham, C.: Volcanic air pollution and human health: recent advances and future directions, *Bull. Volcanol.*, 84, 11, <https://doi.org/10.1007/s00445-021-01513-9>, 2021.

Tam, E., Miike, R., Labrenz, S., Sutton, A. J., Elias, T., Davis, J., Chen, Y.-L., Tantisira, K., Dockery, D., and Avol, E.: Volcanic air pollution over the Island of Hawai'i: Emissions, dispersal, and composition. Association with respiratory symptoms and lung function in Hawai'i Island school children, *Environ. Int.*, 92–93, 543–552, 1375 <https://doi.org/10.1016/j.envint.2016.03.025>, 2016.

US EPA National Center for Environmental Assessment, R. T. P. N.: 2008 Final Report: Integrated Science Assessment (ISA) for Sulfur Oxides – Health Criteria, 2008.

Whitty, R., Pfeffer, M., Ilyinskaya, E., Roberts, T., Schmidt, A., Barsotti, S., Strauch, W., Crilley, L., Pope, F., Bellanger, H., Mendoza, E., Mather, T., Liu, E., Peters, N., Taylor, I., Francis, H., Leiva, X. H., Lynch, D., Nobert, S., and Baxter, P.: Effectiveness of low-cost air quality monitors for identifying volcanic SO₂ and PM downwind from Masaya volcano, 1380 Nicaragua, *Volcanica*, 5, 33–59, <https://doi.org/10.30909/vol.05.01.3359>, 2022.

Whitty, R. C. W., Ilyinskaya, E., Mason, E., Wieser, P. E., Liu, E. J., Schmidt, A., Roberts, T., Pfeffer, M. A., Brooks, B., Mather, T. A., Edmonds, M., Elias, T., Schneider, D. J., Oppenheimer, C., Dybwad, A., Nadeau, P. A., and Kern, C.: Spatial and Temporal Variations in SO₂ and PM_{2.5} Levels Around Kīlauea Volcano, Hawai'i During 2007–2018, *Front. Earth Sci.*, 1385 8, <https://doi.org/10.3389/feart.2020.00036>, 2020.

World Health Organization: WHO global air quality guidelines: particulate matter (PM_{2.5} and PM₁₀), ozone, nitrogen dioxide, sulfur dioxide and carbon monoxide, World Health Organization, xxi, 267 pp., 2021.

Yang, M., Chu, C., Bloom, M. S., Li, S., Chen, G., Heinrich, J., Markeyvych, I., Knibbs, L. D., Bowatte, G., Dharmage, S. C., and others: Is smaller worse? New insights about associations of PM₁ and respiratory health in children and 1390 adolescents, *Environ. Int.*, 120, 516–524, 2018.

Zhang, Y., Ding, Z., Xiang, Q., Wang, W., Huang, L., and Mao, F.: Short-term effects of ambient PM₁ and PM_{2.5} air pollution on hospital admission for respiratory diseases: Case-crossover evidence from Shenzhen, China, *Int. J. Hyg. Environ. Health*, 224, 113418, <https://doi.org/10.1016/j.ijheh.2019.11.001>, 2020.